PROJECT REPORT

On

DESIGN AND FABRICATION OF MULTIFUNCTIONAL CHITOSAN-ACTIVATED CARBON-CLAY NANOCOMPOSITES FOR ENVIRONMENTAL REMEDIATION

Submitted by

FATHIMA SAHVA
(AB23CHE006)

In partial fulfillment for the award of the

Bachelor's Degree in Chemistry

DEPARTMENT OF CHEMISTRY AND CENTRE FOR RESEARCH

ST. TERESA'S COLLEGE (AUTONOMOUS)
ERNAKULAM

2025-2026

DEPARTMENT OF CHEMISTRY AND CENTRE FOR RESEARCH

ST. TERESA'S COLLEGE (AUTONOMOUS)

ERNAKULAM

B.Sc. CHEMISTRY PROJECT REPORT

Name	:	**FATHIMA SAHVA**
Register Number	:	**AB23CHE006**
Year of Work	:	**2025-2026**

This is to certify that the project **"DESIGN AND FABRICATION OF MULTIFUNCTIONAL CHITOSAN-ACTIVATED CARBON-CLAY NANOCOMPOSITES FOR ENVIRONMENTAL REMEDIATION"** is the work done by **FATHIMA SAHVA.**

Dr. Saritha Chandran A.
Head of the Department

Dr. Annu Raju
Staff-member in charge

Submitted to the Examination of Bachelor's Degree in Chemistry

Date: 10/4/26

Examiners: SENJU DEVASYKUTTY, Binoy

: Lintu Anto

DEPARTMENT OF CHEMISTRY AND CENTRE FOR RESEARCH

ST. TERESA'S COLLEGE (AUTONOMOUS)

ERNAKULAM

CERTIFICATE

This is to certify that the project work entitled "**DESIGN AND FABRICATION OF MULTIFUNCTIONAL CHITOSAN-ACTIVATED CARBON-CLAY NANOCOMPOSITES FOR ENVIRONMENTAL REMEDIATION**" is the work done by **FATHIMA SAHVA** under my guidance in the partial fulfilment of the award of the Degree of Bachelor of Science in Chemistry at St. Teresa's College (Autonomous), Ernakulam affiliated to Mahatma Gandhi University, Kottayam.

DR. ANNU RAJU
Assistant Professor,
Department of Chemistry and Centre for Research,
St. Teresa's College (Autonomous), Ernakulam

DECLARATION

I hereby declare that the project work entitled "**DESIGN AND FABRICATION OF MULTIFUNCTIONAL CHITOSAN-ACTIVATED CARBON-CLAY NANOCOMPOSITES FOR ENVIRONMENTAL REMEDIATION**" submitted to Department of Chemistry and Centre for Research, St. Teresa's College (Autonomous) affiliated to Mahatma Gandhi University, Kottayam, is a record of an original work done by me under the guidance of **DR. ANNU RAJU, ASSISTANT PROFESSOR,** Department of Chemistry and Centre for Research, St. Teresa's College (Autonomous), Ernakulam and this project work is submitted in the partial fulfilment of the requirements for the award of the Degree of Bachelor of Science in Chemistry.

FATHIMA SAHVA

Acknowledgements

First of all, I thank **Almighty God** for the successful completion of this project.

I express our heartfelt thanks to my project supervisor **Dr. Annu Raju** Assistant Professor, my guide, St. Teresa's College (Autonomous), Ernakulam, for her guidance, suggestions and encouragement for the successful completion of this project.

I would like to express my gratitude to **Dr. Saritha Chandran A**., Head of the Department of Chemistry and Centre for Research, St. Teresa's College (Autonomous), Ernakulam, for her constant encouragement and motivations.

I take this opportunity to express my sincere thanks to **Prof. Dr. Anu Joseph**, Principal, **Rev. Sr. Nilima CSST**, Manager, and Directors **Rev. Sr. Francis Ann**, and **Rev. Sr. Tessa CSST**, St. Teresa's College (Autonomous), Ernakulam, for being the pillars of support and providing good infrastructure fostering a conductive environment for student's academic growth.

I express my heartfelt thanks to all teachers of the Chemistry Department, for their wholehearted help and advices during the academic year. I also remember the valuable support of the non-teaching staff of the department during chemistry lab hours and the project hours.

I heartily thank **SAIF (Mahatma Gandhi University, Kottayam), STIC (CUSAT)** for providing all the spectroscopic assistance needed for the characterization of the samples within the time limit.

I thank **Department of Zoology** and **Teresian Instrumentation and Consultancy Centre (TICC)** St. Teresa's College, for their support and guidance for my project.

Last, but not least, I'm grateful to our loving families and friends for the care, support and concern they provide to follow my passion.

Fathima Sahva

Contents

Chapter 1 Introduction	**1**
1.1 Environmental Impact of Dye In Human and Aquatic Life	1
1.2 Clay	3
1.2.1 Main Types of Clay Minerals	4
1.2.2 Physical Properties	6
1.2.3 Chemical and Surface Properties	6
1.2.4 Montmorillonite Clay	7
1.3 Chitosan	8
1.4 Activated Carbon	10
1.5 Biopolymer Clay Nanocomposite	11
1.6 Objectives of Current Study	14

Chapter 2 Materials and Methods	**15**
2.1 Work Plan	15
2.2 Experimental Procedure	15
2.2.1 Materials Required	15
2.2.2 Modification of MMT Clay Using CTAB and Cinnamic Acid	15
2.2.3 Modification of MMT Clay Using CTAB	16
2.2.4 Delamination of Activated Carbon	17

2.2.5 Chitosan-Activated Carbon Composite	18
2.2.6 Preparation of Nanocomposite 1	19
2.2.7 Preparation of Nanocomposite 2	20
2.3 Characterisation	21
2.3.1 Characterisation using FT-IR	21
2.3.2 Characterisation using XRD	22
2.3.3 UV-Visible Analysis	23
2.4 Application – Dye Removal	23
2.4.1 Preparation of Dye Solution	23

Chapter 3 Results and Discussion	**25**
3.1 FT-IR Spectroscopy Analysis	25
3.1.1 FT-IR spectrum of pure Na^+-MMT Clay	25
3.1.2 FT-IR spectrum of Modified Cinnamic acid-CTAB-MMT Clay	27
3.1.3 FT-IR spectrum of Modified CTAB-MMT Clay	29
3.1.4 FT-IR spectrum of CTAB-Cinnamic acid -CS/AC Nanocomposite	31
3.1.5 FT-IR spectrum of CTAB-MMT CS/AC Nanocomposite	33
3.2 XRD Analysis	35
3.2.1 XRD analysis of Pure Na^+-MMT clay	35
3.2.2 XRD analysis of Modified clay (MMT-CTAB-Cinnamic acid)	36
3.2.3 XRD analysis of Modified MMT-CTAB clay	37
3.2.4 XRD analysis of MMTCTAB-Cinnamic CS/AC Nanocomposite	38
3.2.5 XRD analysis of MMT CTAB-CS/AC	39

3.3 Evaluation of Dye Adsorption Efficiency	41
3.3.1 UV-Visible Spectrum Analysis of Dye solution	42
3.3.2 UV-Visible Spectrum Analysis of Dye solution treated with MMT-CTAB Cinnamic acid CS/AC Nanocomposite	43
3.3.3 UV-Visible Spectrum Analysis of Dye solution treated with MMT-CTAB CS/AC Nanocomposite	45

Chapter 4 Conclusions	**49**

References	**53**

Chapter 1

Introduction

1.1 ENVIRONMENTAL IMPACT OF DYE IN HUMANS AND AQUATIC LIFE

In a world increasingly threatened by environmental degradation, climate change, and resource scarcity, wastewater treatment has emerged as a crucial, yet often underestimated component of sustainable development. As urban populations continue to expand and industrial activities intensify, the generation of wastewater has reached unparalleled levels, bringing considerable risks to public health, aquatic ecosystems, and global freshwater resources. Wastewater can contain harmful pathogens, chemicals, heavy metals, nutrients, and organic matter that, if released untreated, have detrimental impacts on health and the environment (1).

The most important direct sources of water pollution are the textile, tannery, and paper industries, which consume enormous amounts of water and are responsible for contamination by discharging huge volumes of wastewater into aquatic ecosystems. Their large scale production and widespread applications have caused synthetic organic dyes to permeate different compartments of water and soil environments (2). Dyes have harmful effects on water bodies, as industrial waste is often discharged into rivers and lakes, ultimately causing water pollution. Therefore, quick preventive measures are needed to protect the environment from dye waste (3).

The toxic and carcinogenic effects of untreated textile effluent are well understood (4). Textile effluent, due to its dark colour, usually blocks sunlight and hinders the life of aquatic organisms. The majority of dyes used in the textile industry number approximately ten thousand, of which azo dyes constitute the largest and most recalcitrant category on a commercial scale. The release of these synthetic azo dyes into the environment has detrimental effects on all forms of life.

Textile printing and dyeing processes include pretreatment of fabric, dyeing with synthetic dyes, printing, and finishing steps, and each stage leads to water contamination (5). These textile dyes, which are readily soluble in water, negatively affect fragile ecosystems around industrial areas and represent serious environmental problems (6). Among different pollutants of aquatic ecosystems, dyes form a large and important group of industrial chemicals, with over 700,000 tons of waste produced annually (7). The discharge of textile wastewater containing high colour, suspended solids, and dissolved organics represents a major industrial pollution problem.

Textile wastewaters are usually mixtures of complex particulates, processing assistants, salts, surfactants, acids, and alkalis that vary widely in chemical composition, ranging from inorganic compounds to polymers and organic products. Due to variations in pH, temperature, flow rate, and pollutants, textile wastewater typically requires both physicochemical and biological treatments to meet stringent effluent standards. Various methods for removing organic dyes from water are categorised into chemical, physical, and biological approaches. Physical methods include adsorption, coagulation or flocculation, and filtration. Other available

processes for dye wastewater treatment include chemical oxidation, foam flotation, electrolysis, biodegradation, adsorption, chemical coagulation, and photocatalysis. Among these methods, adsorption onto activated carbon has proven to be one of the most effective and reliable physicochemical treatment technologies (8).

Recent research on montmorillonite (MMT) and chitosan has focused on developing advanced nanocomposite materials with enhanced functional properties. Chitosan–MMT nanocomposite hydrogels have been widely studied for controlled fertilizer release. These systems help regulate nutrient release, reducing leaching and minimising environmental pollution. Beyond agriculture, chitosan–MMT nanocomposites are being explored in food packaging as high-barrier materials to extend shelf life. Also used in environmental remediation for heavy metal and pollutant removal. It has wide applications in biomedical fields such as drug delivery, tissue engineering, and biosensing (9–12) . In our work, in addition to clay and chitosan, we also incorporate activated carbon, CTAB and cinnamic acid, thus enhancing the existing properties.

1.2 CLAY

Clay minerals are essential hydrous aluminium silicate minerals, forming sheet-like structures from weathered rocks, characterized by their fine particle size, plasticity, and ability to hold water and ions, making them vital in soils, sedimentary rocks, and numerous industrial applications like ceramics, drilling, and environmental remediation due to their unique chemical and structural properties (13).

Clay minerals are paying a great deal of attention as potential adsorbents because they possess a highly ordered layered structure, a high ion exchange property, a low cost, and an increased abundance in nature (14),(15).

Clay minerals are classified as Amorphous, Crystalline, three-layer type, regular mixed layer types, and chain-structured type (16).

1.2.1 Main Types Of Clay Minerals

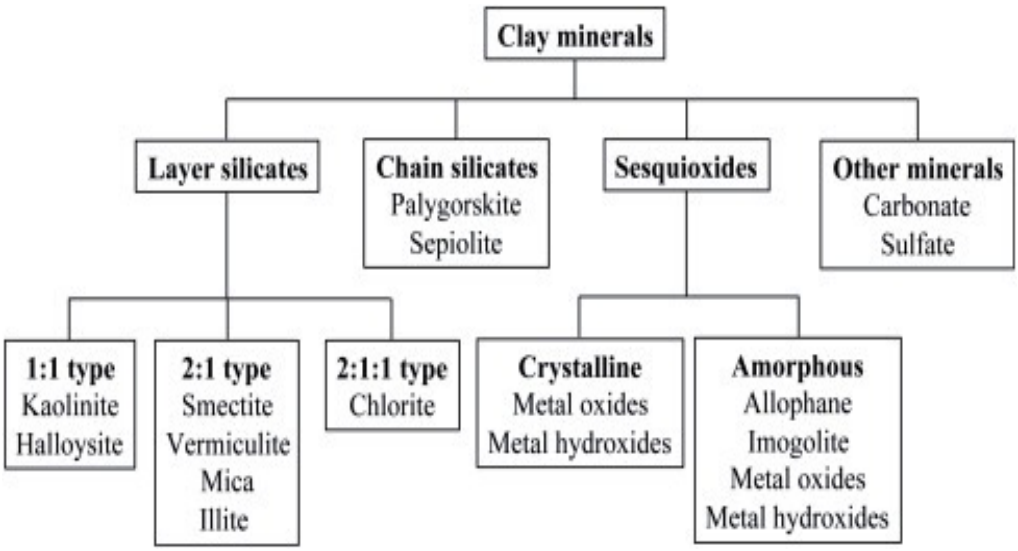

Fig.1.1 Types of Clay

- Kaolinite Group (1:1 Clays): It consists of an alumina octahedral sheet and silica tetrahedral sheet, bonded by strong hydrogen bonds; pure, non-swelling because of the absence of interlayer cations (17),(18). The structural formula for kaolinite is $Al_4Si_4O_{10}(OH)_8$. (16).

Examples: Kaolinite, Halloysite

- Smectite Group (2:1 Clays): It is composed of an octahedral sheet sandwiched between two tetrahedral sheets therefore specified as 2:1 layer mineral (16). The layers are negatively charged, allowing water/ion exchange, leading to significant swelling due to the presence of cations between the layers (17),(19).
  Examples: Montmorillonite (Bentonite), Nontronite, Saponite.

- Illite Group (2:1 Clays): It is a clay mineral mica. Illite is similar to smectite but with potassium ions holding layers tightly therefore having a 2:1 layer, also it prevents the entry of water molecules between the layers making it less expandable (16), (17).
  Examples: Illite, Glauconite.

- Chlorite Group (2:1:1 Clays): A 2:1 layer with an additional hydroxide sheet, giving it distinct properties (16).
  Examples: Clinochlore, Sudoite

- Vermiculite (2:1 Clay): It is a mica- type trioctahedral silicate clay mineral. Each layeres are composed of octahedrally coordinated cations sandwiched by tetrahedrally coordinated cations. High water content and significant swelling capacity (20).

- Serpentine Group (1:1 Clays): Similar structure to kaolinite but magnesium-rich with several polymorphic phases (21).

  Examples: Lizardite, Chrysotile (Asbestos).

1.2.2 Physical Properties

- Plasticity: Ability to deform permanently without cracking when wet, due to water between thin, flexible mineral plates that bind them together (22).
- Dry Strength & Hardness: Becomes strong and hard as it dries or is fired, retaining its moulded shape.
- Shrinkage: Contracts significantly during drying and firing, requiring careful management.
- Texture: Determined by the fineness of its grains (particles < 0.004mm).
- Porosity: Contains pore spaces, influencing water absorption and density.
- Fusing/Vitrification: Fuses into a glass-like, hard ceramic when fired at high temperatures (e.g., in pottery) (23).

1.2.3 Chemical And Surface Properties

- Small Particle Size: Tiny platelets (phyllosilicates) with large surface area (24).
- Cation Exchange Capacity (CEC): Ability to attract and hold positive ions (cations), important for soil fertility and chemistry (25).
- Swelling Potential: Can expand and contract with water absorption/desorption.
- Negative Surface Charge: Particles have a net negative charge, influencing interactions with water and ions (26),(27).
- Adsorption: High capacity to hold substances on its surface (23),(24).

1.2.4 Montmorillonite Clay

Montmorillonite (MMT) is a natural clay with a silicate sheet structure of approximately 1nm thickness. Montmorillonite (MMT), can be effectively used as nanocomposites due to their unique structure and properties (28). MMT has potential adsorption properties for heavy metals because of its high cation exchange capacity. Modification studies on the structure of MMT were introduced to increase the MMT surface area and to generate highly porous materials with improved absorptivity. On addition of water, montmorillonite swells and expands considerably more than the other clays (29). Exfoliation, grafting, surfactant treatment, and polymer crosslinking were introduced as potential techniques to improve the adsorptive properties of MMT. Despite all these attempts, further developments and modifications of MMT structure are still needed to adsorb metal ions potentially. Very recently, a composite of MMT with graphene oxide was fabricated as a strong adsorbent for heavy metals. In this composite, a crosslinking agent was used to implement the combination of graphene oxide with the MMT clay. MMT was utilized to boost the dispersibility of graphene oxide and also to enhance the graphene oxide absorptivity. Thus, it is interesting to combine different carbon sources in a composite structure with MMT and to investigate the removal behavior of the resultant material (30,31).

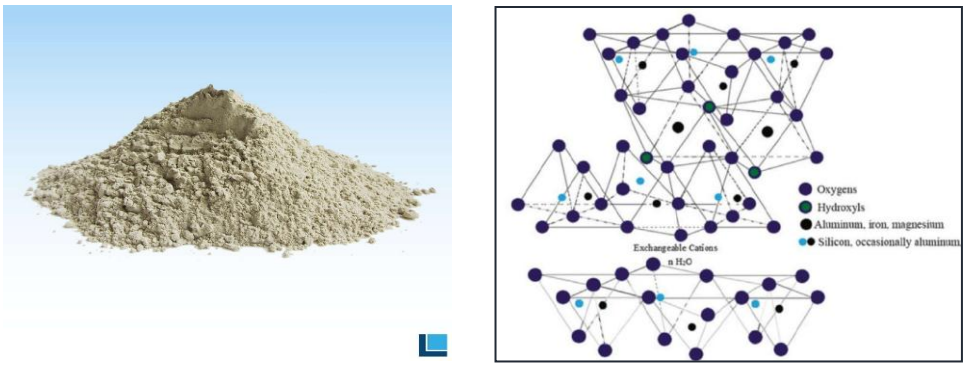

Fig.1.2 Diagram of clay layers and sheets

1.3 CHITOSAN

Nowadays, scientific society is looking forward for biopolymers such as chitosan for good properties in terms of biocompatibility, biodegradability and versatility. They uses these ecofriendly materials due to the insight to reduce the environmental impact that can cause by the regular raw materials (32).

Chitosan is a cationic biopolymer synthesized from chitin, a natural polymer found in the shells of crustaceans such as shrimp, crabs, and lobsters (33). Chitin is the 2nd most abundant natural polymer after cellulose. The exoskeleton of shrimp contains a considerable amount of chitin (34). Chitosan and chitin are composed of varying amount of (β1→4) linked residues of *N*-acetyl-2 amino-2-deoxy-D-glucose and 2-amino-2-deoxy-D-glucose residues (35). Chitosan is a bio-product that is produced from chitin by the partial deacetylation process ,also it is the only polycation in nature. Moreover, chitosan is a renewable natural alkaline polysaccharide which has no side effects on toxicity and also it features good adsorption and moisturizing properties (36).

Chitosan is non-soluble in water , organic solvents and aqueous bases (37). But can easily modified by organic acids, surfactants and polymers(38). The charge density of chitosan depends on degree of acetylation and pH of the media(35) .Chitosan is naturally biodegradable, eco-friendly, bioicompatible and non-toxic material, making it a potent compound of interest (39). Also, it have high chelating ability towards metal ions. There are many chitosan form for biomedical and pharmaceutical applications (37). However, there are more new applications of chitosan in biotechnology(40), wastewater treatment, catalysis, and packaging, which are essential for the future. It should be noted that the wide use of chitosan is due to the presence of hydroxyl and amino groups ,suitable for chemical modifications (32).

Chitosan also contributes to agriculture field using it as coating for seeds, enhancing the propertiesof plants, as plant growth-promoting agent(41) and plant protector. Also used as a food additive, dietary fibre and functional ingredient (32).

The adsorbent properties of chitosan removes heavy metal ions such as Pb^{2+}, Hg^{2+}, and Cu^{2+}, among others from waste water (32). It has a unique chemical structure, which consists of primary amino and primary and secondary hydroxyl functional groups , provides an excellent surface area and a high capability for the uptake of heavy metals , dyes and other contaminants. They exhibit a semi- crystalline structure due to strong intra and intermolecular hydrogen bonding. Chitosan derivatives are produced to enhance or improve their properties like solubility , biodegradability, adsorption capacity, etc (35).

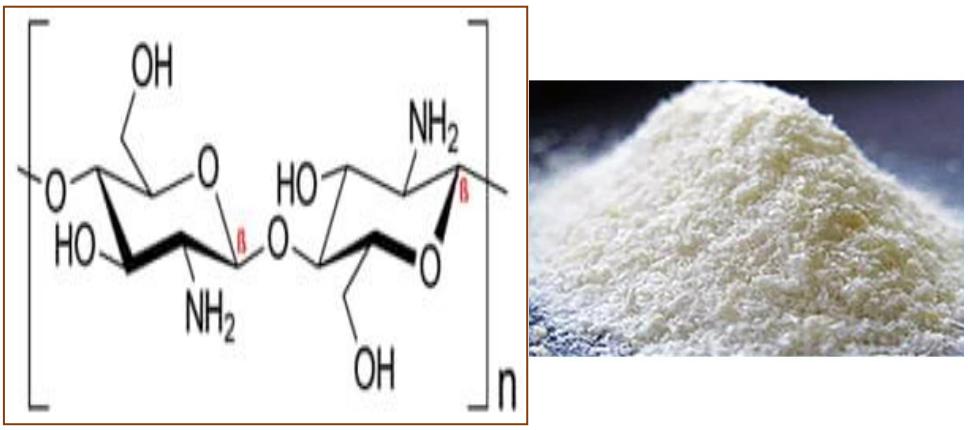

Fig .1.3 Structure of Chitosan

1.4 ACTIVATED CARBON

Activated carbon is a porous carbonaceous material, it's applications in water treatment and desalination is continually expanded (42). It is a common term to describe carbon-based materials that consists of well developed internal pore structure. The properties of AC like high surface area, large porosity, wide spectrum of functional groups present in the surface of AC and internal pore structure consisting of micro, meso and macropores makes AC a multifunctional material which has many applications in vast areas but mainly focused in the environmental field (43). It is widely used for separation and purification. Recent development of AC in fiber form shows increasing applications in various areas due to its unique characteristics (44). Mainly manufacture of AC involves two stages, the carbonization of carbonaceous precursor where most of nanocarbon elements are eliminated and the other stage is activation of resulting char (45). AC is also used as one main adsorbent for desulfurization (46). Atoms that present in carbon structure that are not

carbon but oxygen, nitrogen, hydrogen, sulfur and phosphorus are heteroatoms; surface chemical heterogeneity plays a major role in determining the chemical characteristics of activated carbon which is related to the presence of these heteroatoms (47). Oxidative treatment of AC with nitric acid significantly enhances the specific surface area of activated wood carbon (48). The acidic character of AC surfaces and oxygen containing surface groups are closely related and the chemical nature of the carbon is affected by these groups which are mainly situated in the outer surface or at the edges of the basal plane (47). The adsorption process when we use activated carbon results from the interactions between the carbon surface and the adsorbate (49).

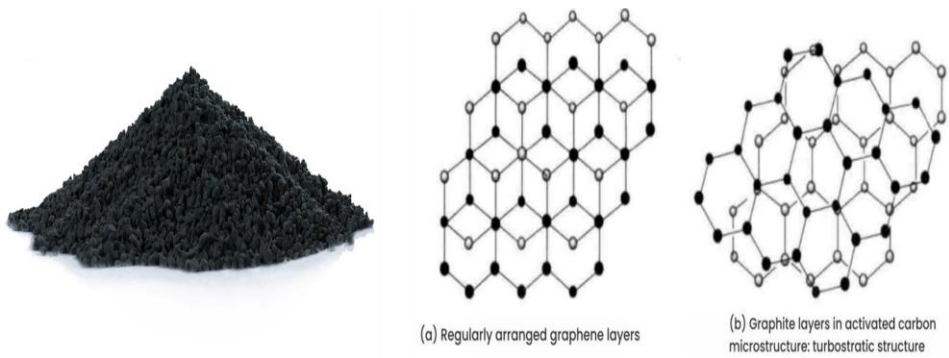

Fig.1.4 Chemical Structure of AC

1.5 BIOPOLYMER CLAY NANOCOMPOSITE

Biopolymer-clay nanocomposites (PCNC) are hybrid materials whose particles are integrated within an organic polymeric matrix. Mean diameter of each particle of one compound is in nano-size range (1–1000 nm) (50). PCNC's have a wide range of rising interest for many applications like to afford materials with function for conductivity,

membranes, corrosion protection and fire retardant behaviour. Most interesting feature of biopolymer clay nanocomposites for many applications like to afford materials with function for conductivity, membranes, corrosion protection and fire retardant behaviour. Most interesting feature of biopolymer clay nanocomposites is the variety of options available in processing because of the dependence on the characteristics of polymer and on the type of interacting mechanism with clay (contains the possibility for preparing thin layers) (51). Their structural or functional behaviour also makes them more interesting (52). Nanocomposites formed by the intercalation of chitosan,a cationic natural polymer, into Na^+ montmorillonite are bidimensional nanostructured materials that contains anionic exchange sites ($-NH_3^+X^-$). This is because of the unique bilayer arrangement of the biopolymer when the amount of intercalated chitosan exceeds the cation exchange capacity (CEC) of the clay (53). PCNCs helps in the removal of heavy metals, dyes, detergents, pesticides and others from contaminated water as it has adsorption property. Adsorption is considered as the most effective technique for the treatment of contaminated water due to its improved accessibility to different adsorbents and also of the ease of operation and low investment costs (54). As PCNC are based on the assembly between polymers and layered nano-sized inorganic fillers, the synergistic interaction between organic and inorganic phases might results rise in materials with new properties (55). Natural biopolymers are filled with layered silicates to enhance their desirable properties while maintaining their biodegradability (56). Their increased mechanical strength, thixotropy, reduced gaseous permeability and higher heat resistance are their advantageous properties which give them a great interest (50). These are also used in material packaging fields. Currently, biopolymers covers approximately 5–10%

packaging (11). Nanocomposites obtained are characterized by chemical and thermal analysis, X-ray diffraction (XRD), Fourier transform infrared (FTIR) spectroscopy, scanning transmission electron microscopy (STEM) and energy-dispersion X-ray analysis (EDX) techniques (52).

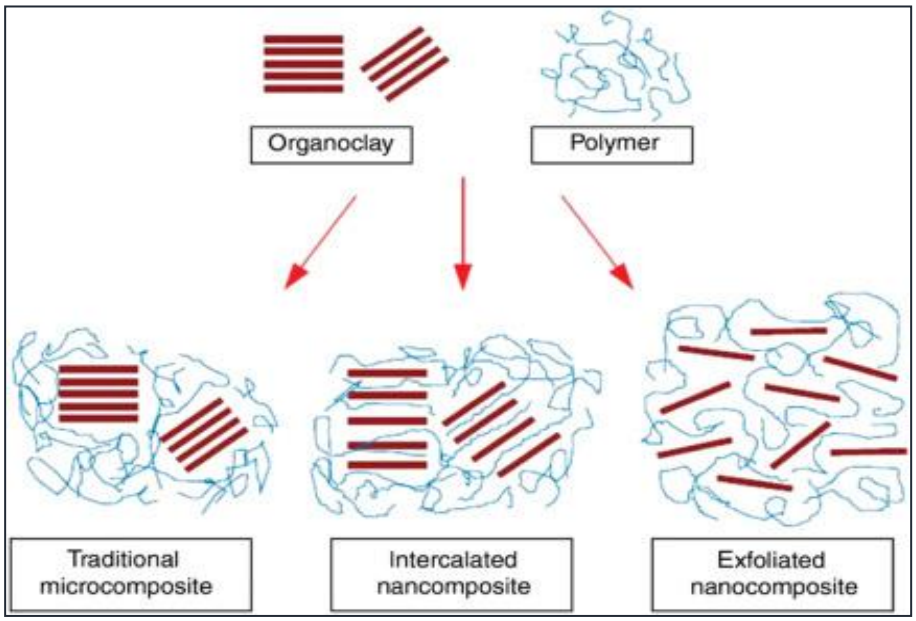

Fig.1.5 Classification of Polymer Clay Nanocomposite

1.6 OBJECTIVES OF CURRENT STUDY

- Modification of MMT clay using Cetyltrimethylammoniumbromide (CTAB) and Cinnamic acid.
- Modification of MMT clay using CTAB only.
- Synthesis of chitosan-activated carbon composite.
- Synthesis of CTAB-Cinnamic acid MMT-CS/AC nanocomposite.
- Synthesis of CTAB MMT-CS/AC nanocomposite.
- To analyse prepared nanocomposites using FT-IR and XRD characterisation techniques.
- To determine the adsorption capacity of the nanocomposites for reactive dyes from wastewater and confirm this via UV-Visible analysis.

Chapter 2

Materials and Methods

2.1 WORK PLAN

The main goals of our project were to prepare two types of biopolymer clay nanocomposites using two different modified MMT clays, which are MMT-CTAB Cinnamic acid CS/AC Nanocomposite and MMT-CTAB CS/AC Nanocomposite. The nanocomposites were characterised using FT-IR and XRD techniques. The dye adsorption capacity of the nanocomposites is also determined by UV-Visible spectroscopy.

2.2 EXPERIMENTAL PROCEDURE

2.2.1 Materials Required

Sodium montmorillonite (MMT) clay, Cetyltrimethylammonium bromide(CTAB), Cinnamic acid, Distilled water, Activated Carbon, Chitosan, 0.1 M Acetic acid, 0.1M KOH.

2.2.2 Modification of MMT Clay Using CTAB and Cinnamic Acid

- Weight of MMT Clay = 4g
- Weight of CTAB = 2.912g
- Weight of Cinnamic acid = 1.1852g
- Total volume of distilled water = 800ml

Fig.2.1 Preparation of Modified MMT-CTAB/Cinnamic acid Clay

Initially, 4g MMT clay is mixed with 200 ml of distilled water for 30 minutes in a magnetic stirrer. To this, 2.912g CTAB, 1.1852g cinnamic acid and 600 ml of distilled water are added and mixed for 48 hours in a magnetic stirrer, then it is centrifuged and dried in an oven.

2.2.3 Modification of MMT Clay Using CTAB

- Weight of MMT clay = 4g
- Weight of CTAB = 2.912g
- Total volume of distilled water = 800ml

Fig.2.2 Preparation of MMT-CTAB Clay

In the initial stage, 4 g of MMT clay is mixed with 200 ml of distilled water and stirred for 30 minutes in a magnetic stirrer. 2.912 g CTAB and 600 ml of distilled water are added to this and stirred for 48 hours in a magnetic stirrer. It is then centrifuged and dried in an oven.

2.2.4 Delamination of Activated Carbon

- Weight of Activated carbon = 4g
- Volume of Distilled water = 100ml

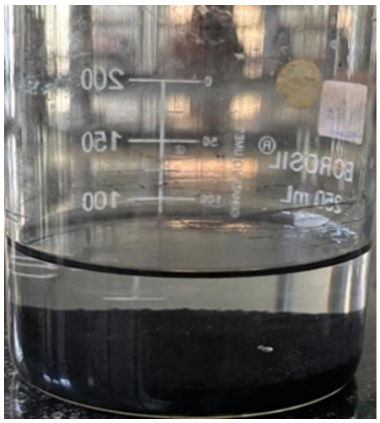

Fig.2.3 Sedimented AC

Fig.2.4 Oven Dried AC

About 4 g of AC was introduced into 100ml distilled water. The resultant suspension was sonicated for an hour. After a sedimentation process of 48 hours, the portion of the supernatant was separated. The remaining sediments of AC was oven dried and weighed. The amount of AC in the supernatant portion was estimated from the difference between the starting AC weight and the sedimented AC weight. The resultant AC was found to be 4.43g.

2.2.5 Chitosan – Activated Carbon Composite

- Weight of Chitosan = 0.1g
- Weight of AC = 1g
- 0.1 M Acetic acid = 100 ml
- 0.1 M KOH

CS/AC nanocomposite was prepared as follows. Firstly, a CS polymer solution was prepared by dispersing 0.1 g of CS in 100ml of 0.1 M acetic acid. The resultant suspension was stirred for 8 hours using a magnetic stirrer to disperse the chitosan completely. Partially protonated chitosan was synthesized by setting the pH at 6.0, utilizing 0.1M KOH. 1g of the delaminated AC was introduced to the CS solution. The blend was then subjected to sonicate for an hour using Branson ultrasonic bath, and then stirred for 8 hrs at 80 °C to graft CS on the surface of AC. The obtained composite was centrifuged and oven-dried.

Fig.2.5 Dried CS-AC Composite

2.2.6 Preparation of Nanocomposite 1

Modified MMT (CTAB-Cinnamic acid) Clay CS-AC Nanocomposite

- Weight of modified clay (CTAB-cinnamic acid) = 0.5g
- Weight of CS/AC composite = 0.5g
- Total volume of distilled water = 50ml

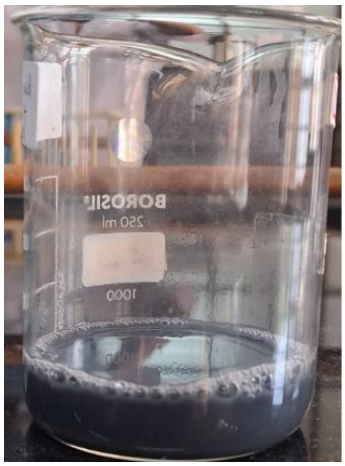

Fig 2.6 Sonicated CS/AC Composite and dried CS/AC Composite

Synthesis was initiated by mixing 0.5 g of modified clay and 0.5 g of CS/AC composite into a beaker containing 50 ml of deionized water and subjected to sonication for 1 hour. The nanocomposite is then centrifuged and dried in an oven.

2.2.7 Preparation of Nanocomposite 2

Modified CTAB MMT Clay CS-AC Nanocomposite

- Weight of modified CTAB-MMT clay = 0.5g
- Weight of CS/AC composite = 0.5g
- Total Volume of distilled water = 50ml

Fig. 2.7 Synthesized CTAB MMT-CS/AC Nanocomposite

The synthesis is conducted same as nanocomposite 1 by mixing 0.5g CTAB modified clay and 0.5g of CS/AC composite into a beaker containing 50ml of deionised water, this is sonicated for one hour. The nanocomposite is then centrifuged and oven-dried.

2.3 CHARACTERISATION

The functional group characterisation and d-spacing between the clay layers of biopolymer clay nanocomposite were investigated through FT-IR and XRD analyses.

2.3.1 Characterisation using FT-IR

The newly prepared nanocomposites are subjected to FT-IR analysis. Using infrared spectroscopy, the molecular vibrations are investigated. Infrared light can only be absorbed by bonds that have varying dipole moment during vibration. The samples of MMT-CS/AC nanocomposites, modified and unmodified MMT clays, were characterised using FT-IR.

The spectrum was obtained using KBr pellets in the 4000cm^{-1} to 400cm^{-1} range. Percent transmittance is plotted against wavenumber. Certain groups inside the molecule produce characteristic absorption bands with wavenumbers that fall within a particular range, regardless of the composition. The wave numbers at which absorption is detected can be used to identify the presence of functional groups. In the current study, the intercalation of the modifiers in the clay was confirmed using infrared data.

2.3.2 Characterisation using XRD

X-ray diffraction is a non-destructive analytical technique for identifying and characterizing the crystalline structure of materials. The technique relies of the principle of diffraction, which happens when the X-rays interact with a crystalline material. The particular arrangement of atoms in the crystal lattice causes the X-rays to scatter in specific directions, thus producing a diffraction pattern that can be recorded and analyzed. X-ray refraction uses the dual wave/particle duality of X-rays. This technique's primary use is the identification and characterization of substances according to the pattern of their diffraction. XRD is a potent analytical method for figuring out the interlayer spacing, phase composition and crystalline structureof nanocomposites. The reflected X-ray intensity plotted against 2θ values in the XRD graph.

Where θ is the angle at which the X-ray strikes the sample and n is the order of reflection. Monochromatic X-ray wavelength is denoted by λ, while d represents the separation between two comparable planes. The d-spacing can be calculated using Bragg's equation. In the present study, the intercalation of clay was assessed by utilizing XRD to determine the angle of diffraction and d-spacing values.

2.3.3 UV-Visible Analysis

In the electromagnetic spectrum's visible (VIS) and ultraviolet UV) regions, which range from 200 to 800 nm, most organic compounds and functional groups exhibit little to no light absorption, making absorption spectroscopy ess effective in this area. However, insights can occasionally be gained from these spectral regions. By integrating this information with data obtained from infrared spectroscopy, significant structural insights can be uncovered. This concept is derived from Beer-Lambert's Law. When energy is absorbed by electrons in both bonded and unbonded molecules, they transition to higher energy states, and there are four main types of transitions: π -π *, σ – σ *, n- σ *, and n- π *. The hierarchy of energy for these transitions is as follows: σ - σ * > n- σ * > π - π* > n- π*. Absorption in the 200-260 nm range is attributed to the transitions, while n- π * transitions are responsible for absorption in the 350-400 nm range. Ultraviolet-visible spectroscopy was conducted within the 200 to 700 nm range.

2.4 APPLICATION – DYE REMOVAL

2.4.1 Preparation of Dye Solution

In order to create a 10 ppm Alizarin Red dye solution, 10 mg of Alizarin Red dye was first dissolved in 100 ml of distilled water to create a stock solution with a 100 ppm concentration. The stock solution was then utilized to make the required 10 ppm solution. Precisely, 10 ml of the 100 ppm dye solution was quantified and further diluted to a total volume of 100 ml with distilled water, creating a 10 ppm dye solution. To study adsorption, 50 mg of each of the synthesized nanocomposites was meticulously weighed and introduced into 50 ml of the prepared 10 ppm

dye solution. The solution was left to react for a period of 45 minutes in total to test the efficiency of nanocomposite dyes in dye removal.

Fig.2.8 Dye nanocomposite interaction

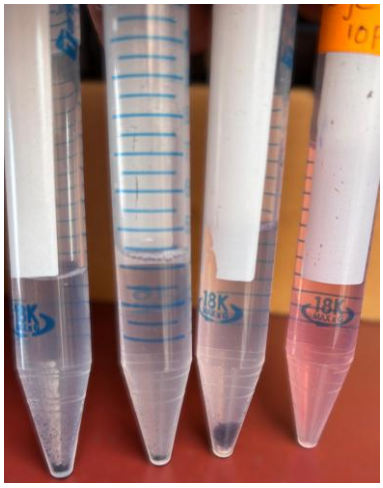

Fig.2.9 Sample for analysis

Monitoring of the process of adsorption was conducted via analysis of dye solution samples utilizing UV-visible spectrophotometry every 15-minute interval. This spectroscopic study assisted in the determination of the reduction in dye concentration with time, thus evaluating the adsorption capacity and efficiency of the nanocomposites in the removal of the dye from the solution.

Chapter 3

Results and discussion

3.1 FT-IR SPECTROSCOPY ANALYSIS

The FT-IR spectrum of the pure Na^+- MMT, CTAB-Cinnamic acid MMT clay, CTAB -MMT Clay, MMT-CTAB Cinnamic CS/AC nanocomposite, MMT-CTAB CS/AC Nanocomposite are analysed. The FT-IR absorption bands were confirmed in every instance by analysing the characteristic bands.

3.1.1 FT-IR spectrum of pure Na^+-MMT clay

The FT-IR spectrum of pure Na^+- MMT clay is shown in the Fig.3.1.
In pure Na^+-MMT clay, a broad band at 3455.11cm^{-1} indicates the -OH stretching of water molecules in the interlayer of the clay. The band at 3629.21 cm^{-1} represents the -OH stretching of the Al-OH bond. The band observed at 1637.36cm^{-1} corresponds to the -OH bending vibration of the Al-OH bond. The band observed at 1637.36cm^{-1} corresponding to the -OH bending vibration of water molecules in the interlayer of the clay. The band identified at 1640.16cm^{-1} represents the Si-O-Si stretching vibration and the bands at 524.22cm^{-1} and 463.92cm^{-1} are identified as the Al-O-Si and Si-O-Si bending vibrations respectively. The band observed at 916.01cm^{-1} which belongs to the bending vibration of Al-OH.

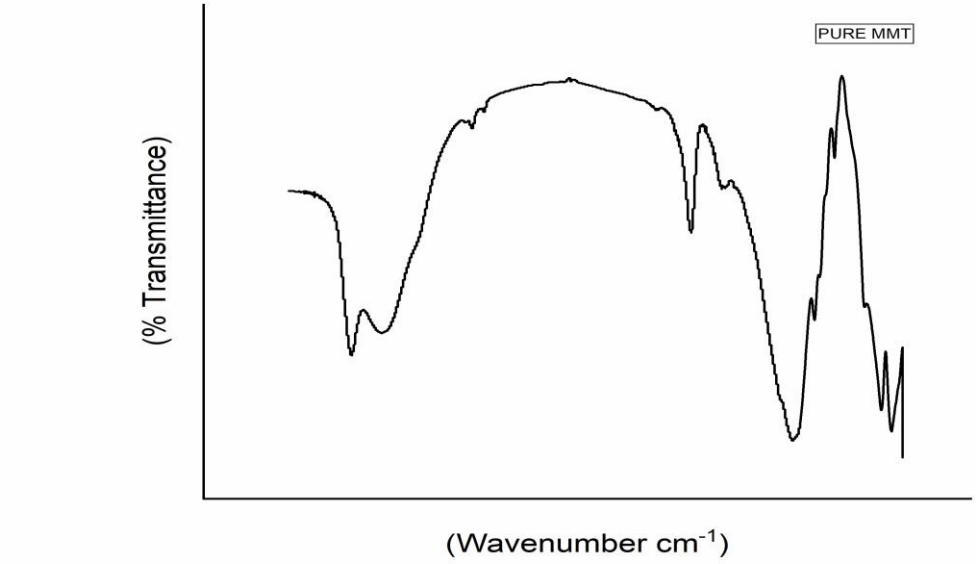

Fig.3.1 FT-IR of Pure Na^+-MMT Clay

The vibrational frequencies of the peaks are listed in below table 3.1

Table 3.1 Vibrational frequencies of Pure Na^+-MMT clay

Wavenumber (cm^{-1})	Vibration
3629.21	-OH stretching for Al-OH
3455.11	-OH stretching of water
1637.36	-OH bending of water
1640.16	Si-O-Si stretching
916.01	Al-OH bending
524.22	Al-O-Si bending
463.92	Si-O-Si bending

3.1.2 FT-IR SPECTRUM OF MODIFIED CINNAMIC ACID - CTAB -MMT CLAY

The FT-IR spectrum of cinnamic acid–CTAB–MMT is shown in the figure 3.2 . The characteristic bands observed in pure Na^+–MMT clay were also present in the cinnamic acid–CTAB–MMT composite. In this study, FT-IR analysis was used to investigate the possible interactions among the components of the CTAB–MMT composite.

The bands observed at 2919.98 cm^{-1} and 2850.87 cm^{-1} correspond to the asymmetric and symmetric C–H stretching vibrations of the alkyl chains of CTAB, confirming the presence of the organic surfactant within the MMT clay layers. The bands at 3628.64 cm^{-1} and 3015.53 cm^{-1} are attributed to O–H stretching vibrations. The intensity of these bands decreases in cinnamic acid–CTAB–MMT due to the replacement of interlayer water molecules by the hydrophobic surfactant.

The band at 1636.45 cm^{-1} is assigned to the H–O–H bending vibration of absorbed water molecules. The band at 1011.50 cm^{-1} corresponds to Si–O–Si stretching vibrations. The bands at 448.44 cm^{-1} and 517.08 cm^{-1} are attributed to Si–O–Si and Al–O–Si bending vibrations, respectively. The band at 909.38 cm^{-1} is assigned to the bending vibration of Al–OH groups.

Additionally, the band at 1705.49 cm^{-1} corresponds to the C=O stretching vibration of the carboxylic acid group. The band at 1636.45 cm^{-1} is also associated with the C=C stretching vibration of cinnamic acid, while the band at 1576.20 cm^{-1} is attributed to aromatic ring stretching. The band at 1449.27 cm^{-1} corresponds to in-plane O–H bending and C–O stretching vibrations

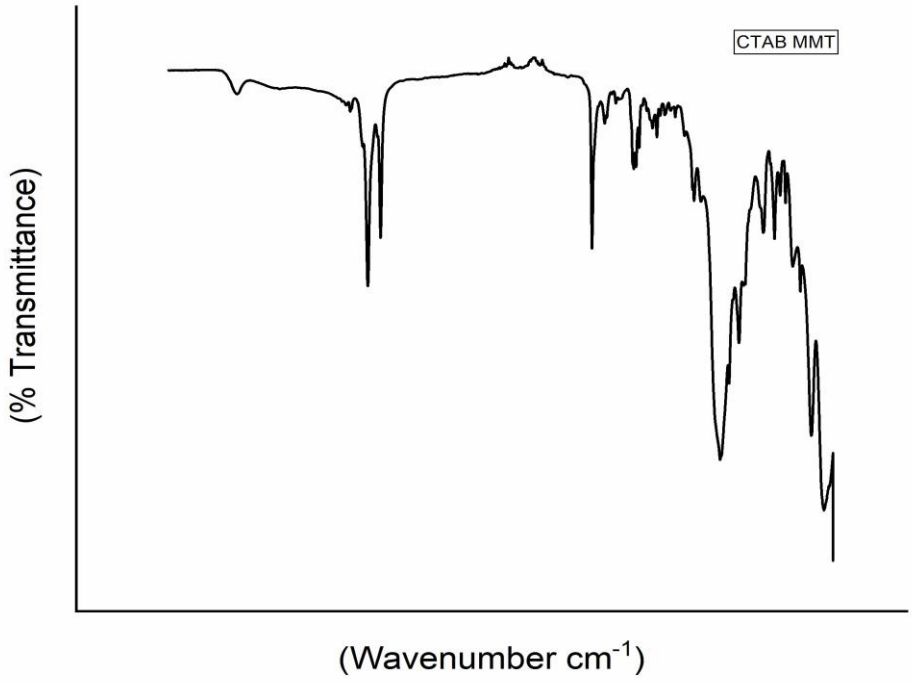

Fig.3.2 FT-IR of Modified MMT clay 1

The vibrational frequencies of the peaks are listed in the table 3.2

Table 3.2 Vibrational frequencies of Modified MMT Clay 1

Wavenumber (cm^{-1})	**Vibration**
3628.64	-OH stretching
1011.50	Si-O-Si stretching
2919.98	Asymmetric C-H_3 stretching of CTAB
2850.87	Symmetric C-H_2 stretching of CTAB
1705.49	C=O stretching of carboxylic acid
1636.45	H-O-H bending of absorbed water
517.08	Al-O-Si bending
448.44	Si-O-Si bending

3.1.3 FT-IR SPECTRUM OF MODIFIED CTAB – MMT CLAY

The FT-IR spectrum of CTAB-MMT is shown in Figure 3.3. The characteristic absorption bands of pure Na^+-MMT clay were also observed in the CTAB-modified MMT, indicating that the clay structure was retained after modification. In this study, FT-IR analysis was employed to investigate the possible interactions between CTAB and MMT in the composite. The bands at 2916.20 cm^{-1} and 2848.50 cm^{-1} correspond to the asymmetric and symmetric C–H stretching vibrations of the alkyl chains of CTAB, confirming the successful incorporation of the organic surfactant into the MMT interlayers. The bands observed at 3626.95 cm^{-1} and 3017.01 cm^{-1} are attributed to –OH stretching vibrations. A decrease in the intensity of these bands in CTAB-MMT suggests that the hydrophobic surfactant partially replaces the interlayer water molecules. The band at 1634.81 cm^{-1} is assigned to the H–O–H bending vibration of adsorbed water. The strong absorption band at 1011.29 cm^{-1} corresponds to Si–O–Si stretching vibrations. The bands at 444.31 cm^{-1}, 417.30 cm^{-1}, and 518.29 cm^{-1} are attributed to Si–O–Si and Al–O–Si bending vibrations, while the band at 910.96 cm^{-1} is associated with the bending vibration of Al–OH groups.

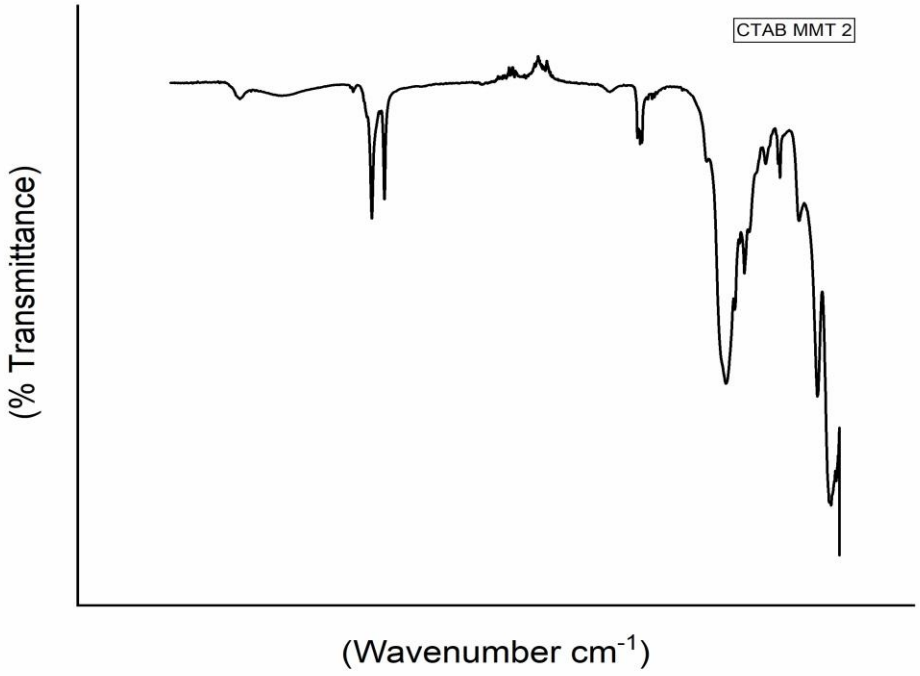

Fig.3.3 FT-IR of Modified MMT Clay 2

The vibrational frequencies of the peaks are listed in below table 3.3

Table 3.3 Vibrational frequencies of Modified MMT Clay 2

Wavenumber (cm^{-1})	Vibration
3626.95	-OH stretching
1011.29	Si-O-Si stretching
2916.20	Asymmetric C-H_3 stretching of CTAB
2848.50	Symmetric C-H_2 stretching of CTAB
1634.81	H-O-H bending of absorbed water
518.29	Al-O-Si bending
444.31	Si-O-Si bending

3.1.4 FT-IR SPECTRUM OF CTAB-CINNAMIC ACID – CS/AC NANOCOMPOSITE

The FT-IR spectrum of the MMT–CTAB–cinnamic acid–CS/AC composite is presented in the figure 3.4. The characteristic absorption bands of pristine Na^+-MMT clay are also observed in the MMT–CTAB–cinnamic acid–CS/AC composite, indicating that the clay structure is preserved after modification. FT-IR analysis was employed to investigate the possible interactions among cinnamic acid, CTAB-modified MMT, and the CS/AC composite. The absorption band at 3627.36 cm^{-1} corresponds to the stretching vibrations of structural –OH groups of MMT clay. The broad band observed at 3339.22 cm^{-1} is attributed to O–H and N–H stretching vibrations, arising from adsorbed water molecules and the amino groups of chitosan. The bands at 2921.75 cm^{-1} and 2850.26 cm^{-1} are assigned to the asymmetric and symmetric stretching vibrations of $–CH_2$ groups, respectively, mainly originating from CTAB alkyl chains and chitosan. The band at 1637.14 cm^{-1} is attributed to C=C stretching vibrations of the aromatic ring of cinnamic acid. The absorption band at 1547.21 cm^{-1} corresponds to N–H bending vibrations (amide II) of chitosan. The bands observed at 1467.05 cm^{-1} and 1377.73 cm^{-1} are assigned to C–H bending vibrations. The characteristic band at 1003.88 cm^{-1} is associated with C–O–C stretching vibrations of chitosan, while the band at 511.39 cm^{-1} corresponds to Si–O–Al bending vibrations of the MMT clay.

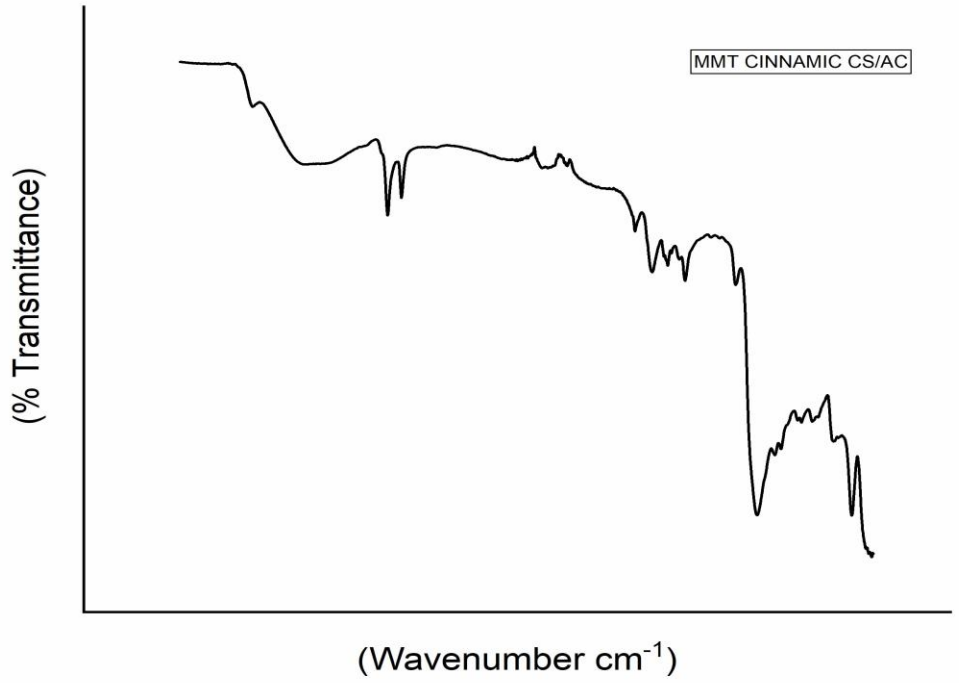

Fig.3.4 FT-IR of MMT- CS/AC Nanocomposite 1

The vibrational frequencies of the peaks are listed in below table 3.4

Table 3.4 Vibrational frequencies of MMT-CS/AC Nanocomposite 1

Wavenumber (cm^{-1})	**Vibration**
3627.36	-OH stretching for MMT Clay
3339.22	N-H stretching of amino group of chitosan
2921.75	Asymmetric C-H_3 stretching of CTAB
1637.14	C=C stretching of aromatic ring
1547.21	N–H bending vibrations of Chitosan
1467.05	C–H bending vibrations
1003.88	C–O–C stretching vibrations of chitosan
511.39	Si–O–Al bending vibrations

3.1.5 FT-IR SPECTRUM OF CTAB-MMT CS/AC NANOCOMPOSITE

The FT-IR spectrum of the MMT–CTAB–CS/AC composite is presented in the figure 3.5. Characteristic absorption bands of pure Na^+-MMT clay were also observed in the MMT–CTAB–CS/AC composite, indicating the preservation of the clay structure after modification. In this study, FT-IR analysis was employed to investigate the possible interactions between the components of CTAB-modified MMT and the CS/AC composite. The absorption band at 3623.31 cm^{-1} corresponds to the O–H stretching vibrations of MMT clay. The bands observed at 2921.04 cm^{-1} and 2849.21 cm^{-1} are attributed to the asymmetric and symmetric stretching vibrations of the $–CH_2$ groups, respectively. The band at 1467.35 cm^{-1} is assigned to C–H bending vibrations. The characteristic band at 1000.77 cm^{-1} represents the C–O–C ring vibrations of chitosan, while the band observed at 511.14 cm^{-1} is associated with Si–O–Al bending vibrations of MMT clay.

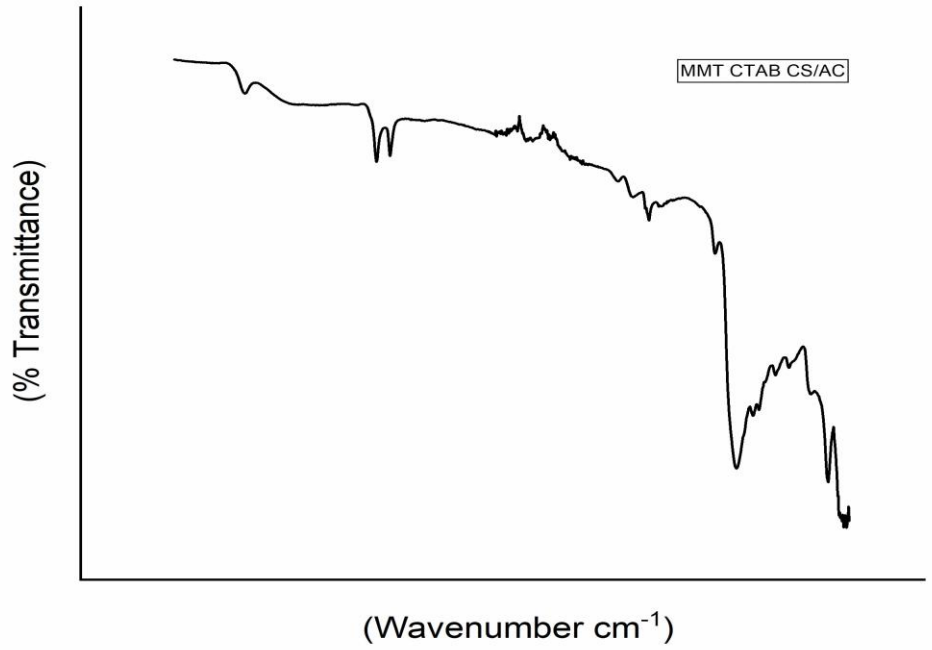

Fig.3.5 FT-IR of MMT- CS/AC Nanocomposite 2

The vibrational frequencies of the peaks are listed in the table 3.5

Table 3.5 Vibrational frequencies of MMT-CS/AC Nanocomposite 2

Wavenumber (cm^{-1})	**Vibration**
3623.31	-OH stretching for MMT Clay
2921.04	Asymmetric C-H_3 stretching of CTAB
2849.21	symmetric C-H_2 stretching of CTAB
1467.35	C–H bending vibrations
1000.77	C–O–C ring vibrations of chitosan
511.14	Si–O–Al bending vibrations

3.2 XRD ANALYSIS

The degree of intercalation/exfoliation can be determined by observing the position, shape and intensity of the XRD peak for MMT CS/AC nanocomposites. We observed the change in (001) reflection peak in each graph. The d-spacing were calculated by considering the (001) reflection.

3.2.1 XRD analysis of Pure Na^+- MMT clay

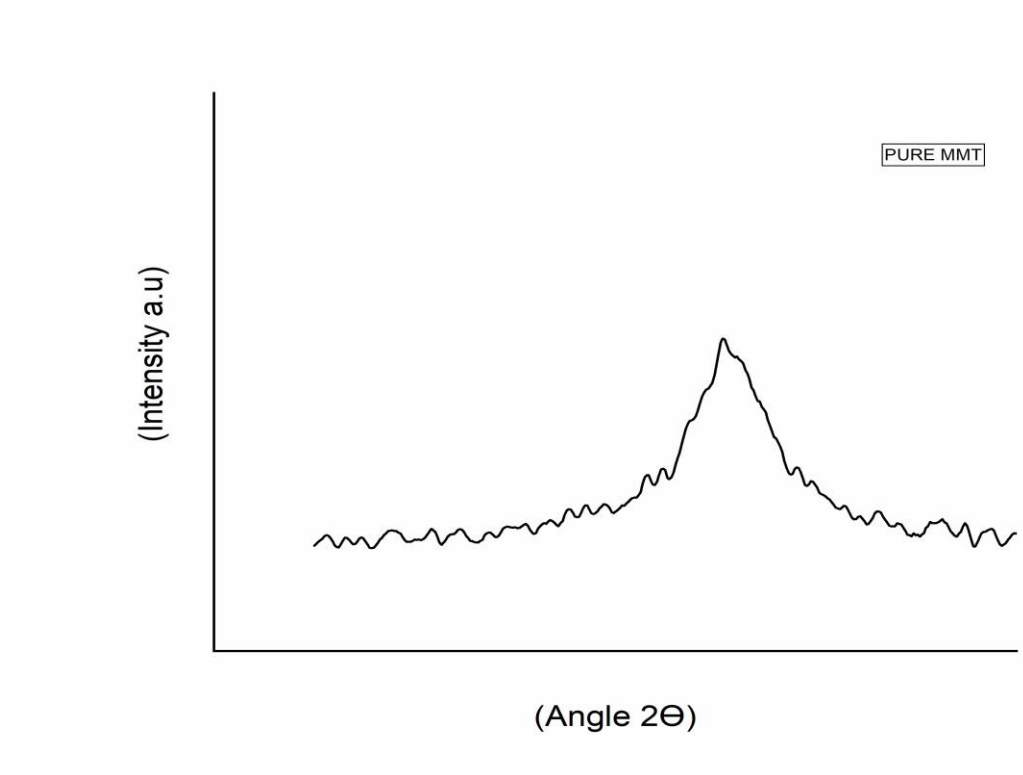

Fig.3.6 XRD of Pure Na^+-MMT clay

Table 3.6 d-spacing of Pure Na^+-MMT clay

SAMPLE	ANGLE 2θ (degree)	d-SPACING (Å)
Pure MMT clay	7.081	12.47

3.2.2 XRD analysis of Modified clay (MMT+CTAB+Cinnamic acid)

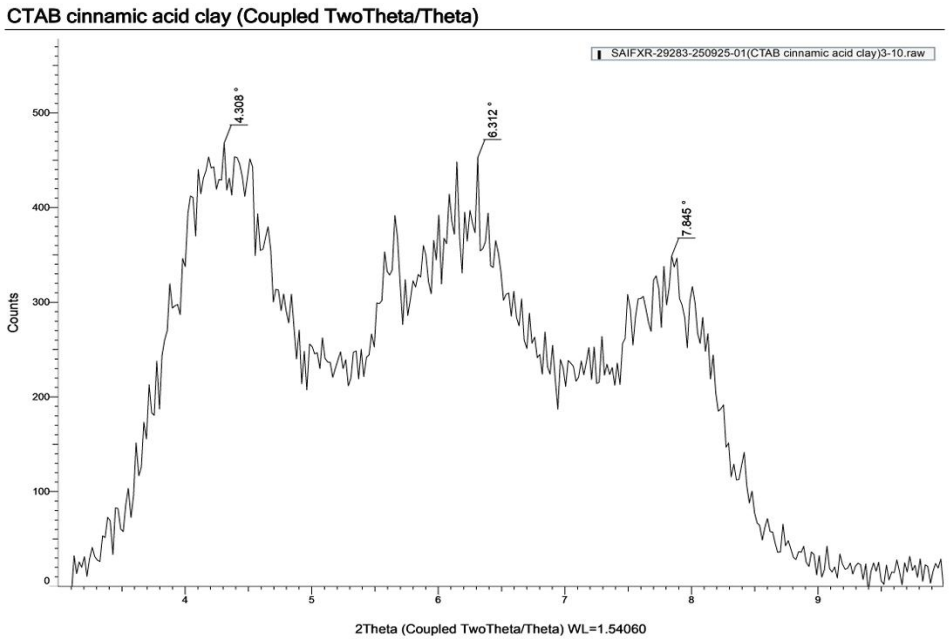

Fig.3.7 XRD of Modified MMT Clay 1

Table 3.7 d-spacing of Modified MMT clay 1

SAMPLE	ANGLE 2θ (degree)	d-SPACING (Å)
MMT-CTAB/cinnamic clay	4.308	20.49266

3.2.3 XRD analysis of Modified MMT-CTAB clay

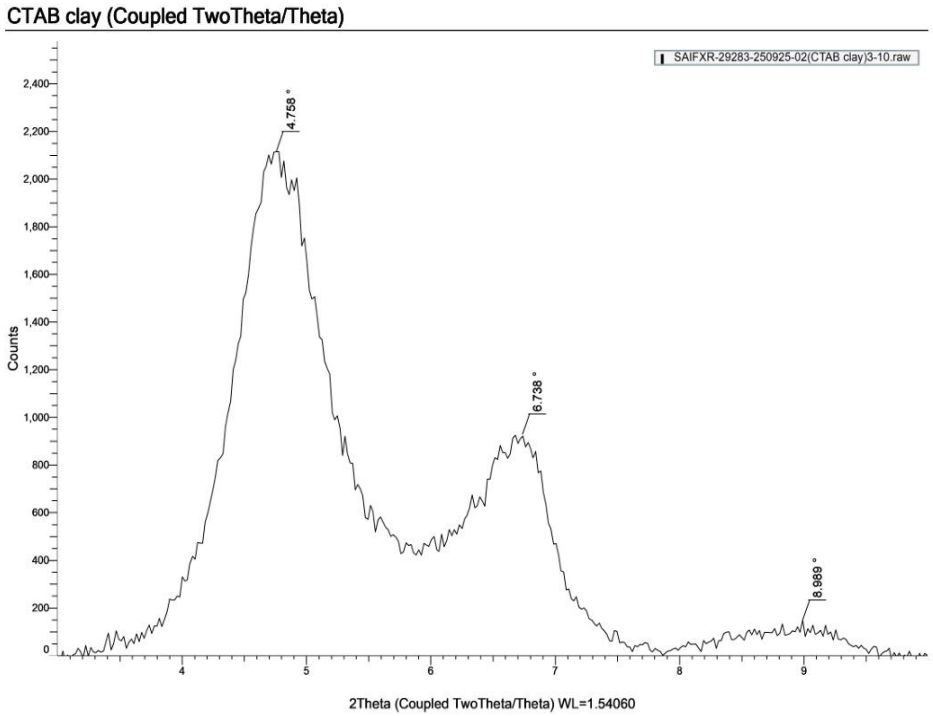

Fig.3.8 XRD of Modified MMT Clay 2

Table 3.8 d-spacing of Modified MMT clay 2

SAMPLE	ANGLE 2θ (degree)	d-SPACING (Å)
MMT-CTAB clay	4.758	18.55908

3.2.4 XRD Analysis of MMT CTAB-Cinnamic CS/AC Nanocomposite

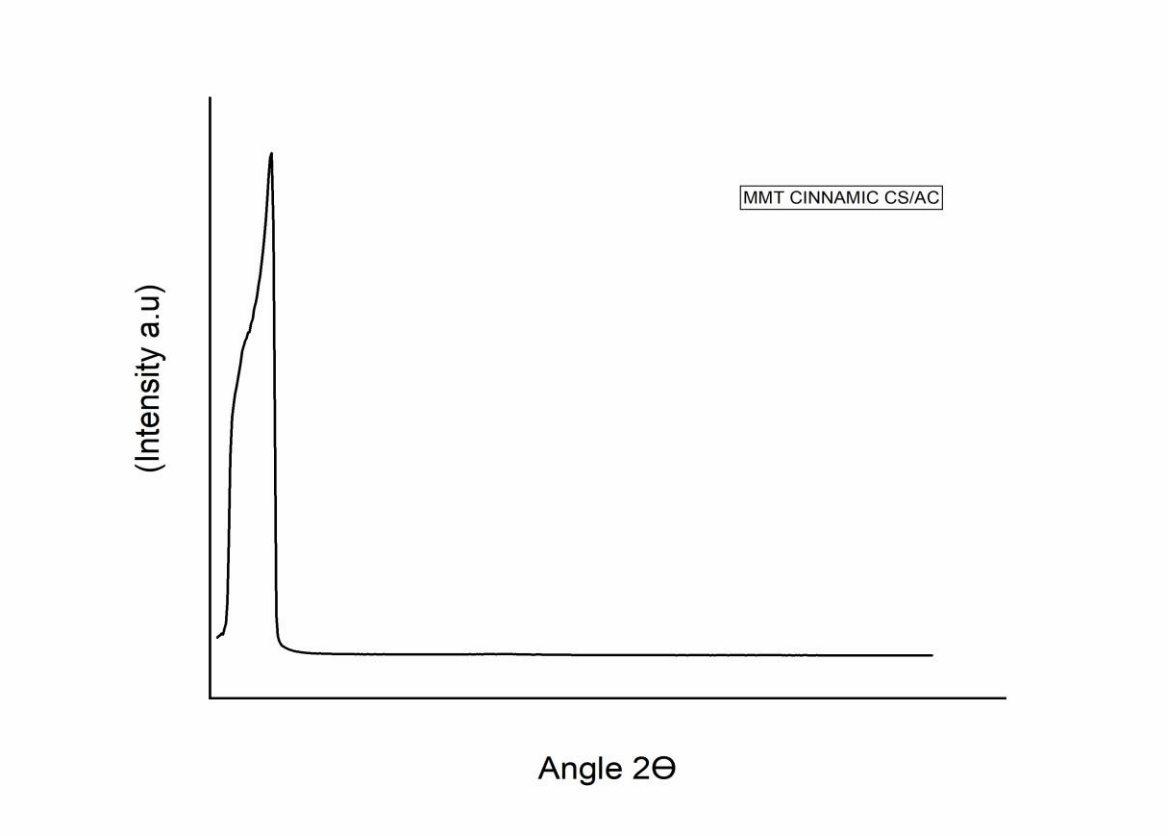

Fig.3.9 XRD of MMT CTAB-Cinnamic CS/AC Nanocomposite

Table 3.9 d-spacing of MMT CTAB-Cinnamic CS/AC Nanocomposite

SAMPLE	ANGLE 2θ (degree)	d-SPACING (Å)
MMT CTAB-Cinnamic CS/AC	0.848	104.14450

3.2.5 XRD Analysis of MMT CTAB- CS/AC Nanocomposite

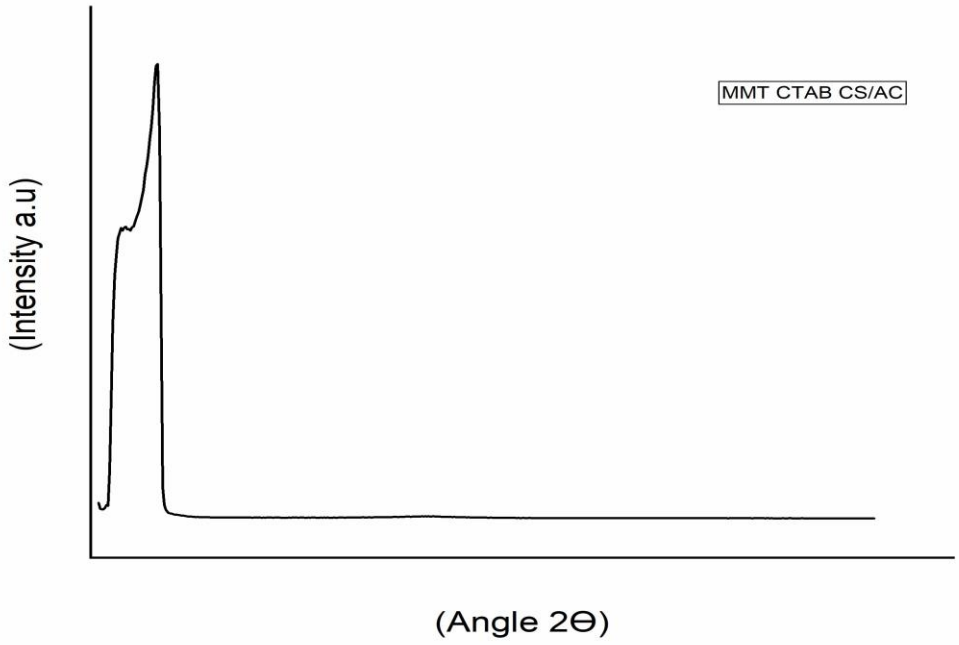

Fig.3.10 XRD of MMT CTAB CS/AC Nanocomposite

Table 3.10 d-spacing of MMT CTAB CS/AC Nanocomposite

SAMPLE	ANGLE 2θ (degree)	d-SPACING (Å)
MMT CTAB CS/AC	0.843	104.70430

On comparing all the (001) reflection peaks of the pure clay, modified clays and MMT CS/AC nanocomposites, table 3.11 is listed.

Table 3.11 Comparison of d-spacing of Pure clay, modified clays and MMT CS/AC nanocomposites.

SAMPLE	ANGLE 2θ (degree)	d-SPACING (Å)
Pure MMT clay	7.081	12.47
Modified clay 1	4.308	20.49266
Modified clay 2	4.758	18.55908
MMT CTAB-Cinnamic CS/AC	0.848	104.14450
MMT CTAB CS/AC	0.843	104.70430

X-ray diffraction is the commonly used technique to calculate the diffraction of nano clay. The d-spacing is calculated using the diffraction peaks in the XRD patterns which is given by Bragg's equation $\lambda = 2d\sin\theta$ where λ is the wavelength, d corresponds to interplanar spacing and θ is the position of diffraction. During incorporation of nano clay into the matrix, the polymer will force the platelets apart causing the diffraction peaks to shift to a lower angle.

Table 3.11. displays the XRD patterns of pure Na^{+}-MMT clay, modified clays and MMT CS/AC nanocomposites. Here, by comparison with pure MMT clay, the d-spacing of modified clay increases from 12.47Å to 20.49Å and 18.55Å.

In modified clay 1, the d-spacing increased from 12.47Å to 20.49Å due to intercalation of CTAB and Cinnamic acid into the clay layers. Thus, the successful modification of clay with CTAB and cinnamic acid.

In modified clay 2, the d-spacing increased from 12.27Å to 18.55Å due to the intercalation of CTAB into the clay layers. Thereby, successful intercalation of clay with CTAB. So, Modified clay 1 contains increased d- spacing which shows the enhanced interlayer spacing.

In comparing the nanocomposites with their corresponding modified clay, both the nanocomposites show a large increase in d-spacing. Comparing MMT CTAB-Cinnamic acid CS/AC nanocomposite with the Modified clay 1, the d-spacing values are 20.49Å to 104.144Å, there is a significant increase in the d-spacing, which shows the exfoliation of the clay layers.
When comparing MMT CTAB-CS/AC nanocomposite with Modified clay 2 the d-spacing values are 18.55Å to 104.704Å. here also the d-spacing values have an extensive increase, which shows the exfoliation of clay layers.

3.3 EVALUATION OF DYE ADSORPTION EFFICIENCY

To assess the performance of the prepared nanocomposites in eliminating dye contaminants from a solution, an adsorption efficiency test is performed. The process starts with the preparation of a 10ppm dye solution. The prepared nanocomposite is subsequently introduced into the dye solution, mixed well, and left to incubate for 45 minutes, allowing the nanocomposite to interact with dye molecules. The adsorption capacity of the nanocomposite is determined via a UV-Visible spectrometer with readings every 15 minutes to track the reduction in the concentration of dye over time. Through a determination of the adsorption value recorded by the spectrometer, the percentage of dye removal can be computed,

showing the adsorption capacity of the nanocomposite and revealing its use in wastewater treatment.

3.3.1 UV - Visible Spectrum Analysis of Dye Solution

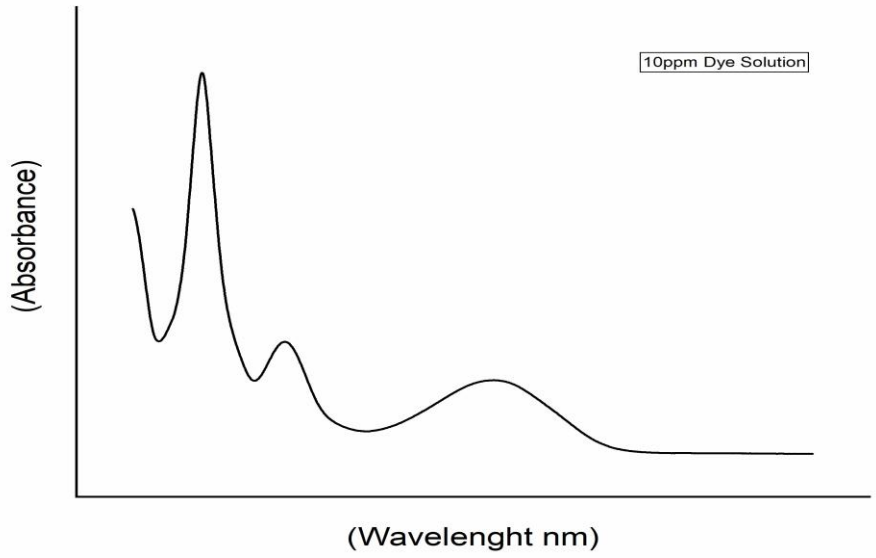

Fig.3.11 UV Visible Spectrum of Dye solution

Table 3.12 UV Visible Analysis of Alizarin Red Dye Solution

SAMPLE	WAVELENGTH (nm)	ABSORBANCE
Alizarin Red Dye	260	0.9407

3.3.2 UV-Visible Spectrum Analysis of Dye Solution Treated with MMT-CTAB Cinnamic acid CS/AC Nanocomposite

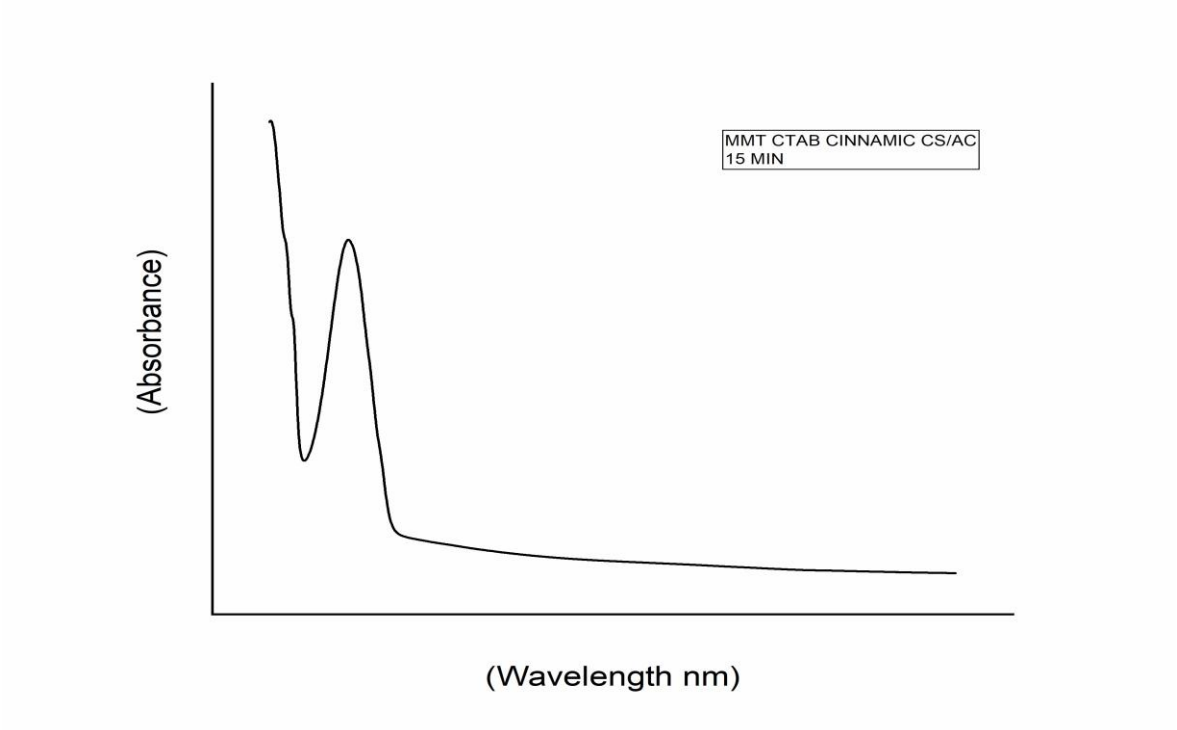

Fig.3.12 UV Visible spectrum of dye solution in MMT CTAB Cinnamic CS/AC Nanocomposite for 15 Min

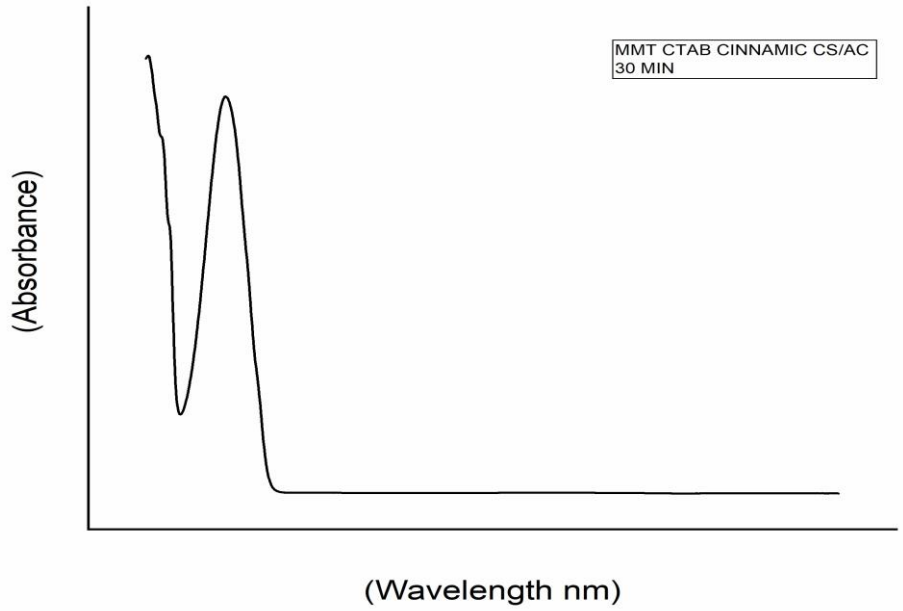

Fig.3.13 UV Visible spectrum of dye solution in MMT CTAB Cinnamic CS/AC Nanocomposite for 30 Min

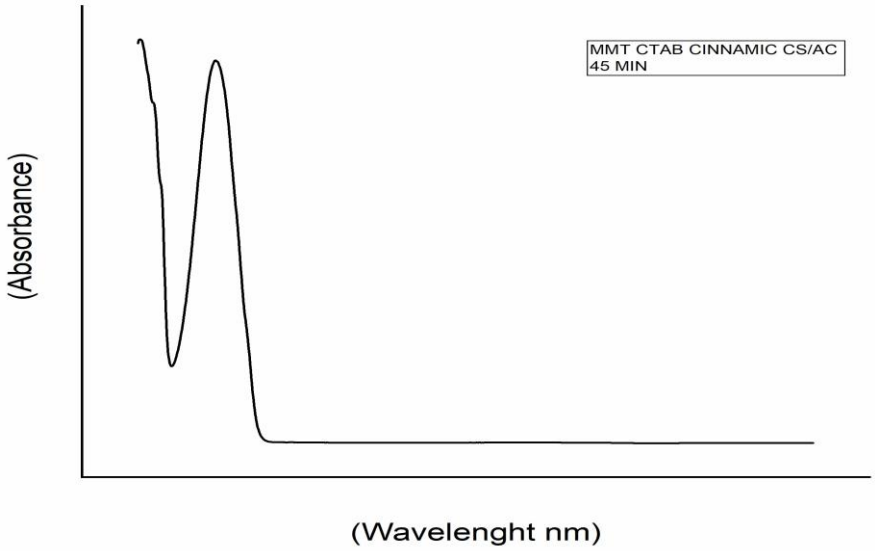

Fig.3.14 UV Visible spectrum of dye solution in MMT CTAB Cinnamic CS/AC Nanocomposite for 45 Min

Table 3.13 UV Visible Analysis of Dye solution in MMT-CTAB Cinnamic CS/AC nanocomposite at different time intervals

Sample	Wavelength (nm)	Absorbance
MMT-CTAB Cinnamic CS/AC for 15 Min	260	2.3646
MMT-CTAB Cinnamic CS/AC For 30 Min	260	2.5375
MMT-CTAB Cinnamic CS/AC For 45 Min	260	2.7794

3.3.3 UV -Visible Spectrum Analysis of Dye Solution Treated with MMT -CTAB CS/AC Nanocomposite

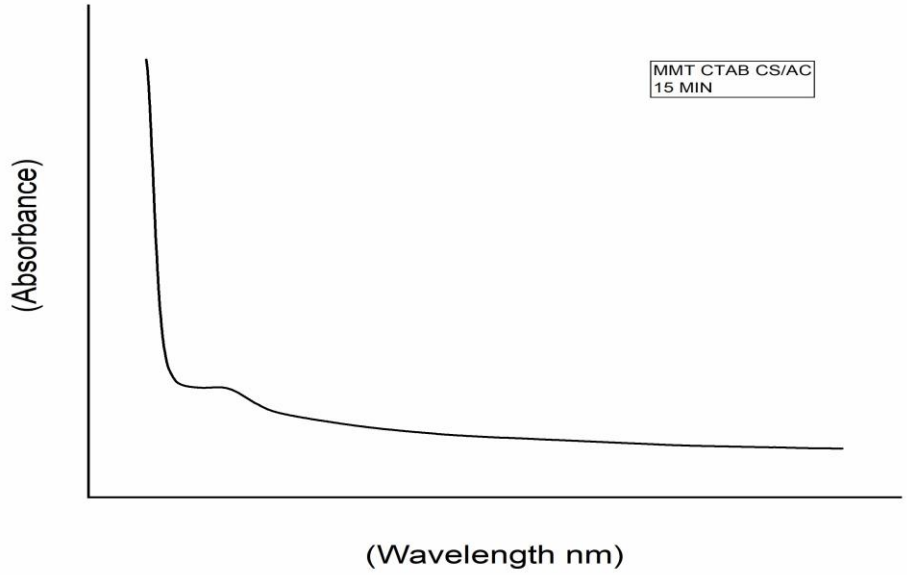

Fig. 3.15 UV Visible spectrum of dye solution in MMT CTAB CS/AC Nanocomposite for 15 Min

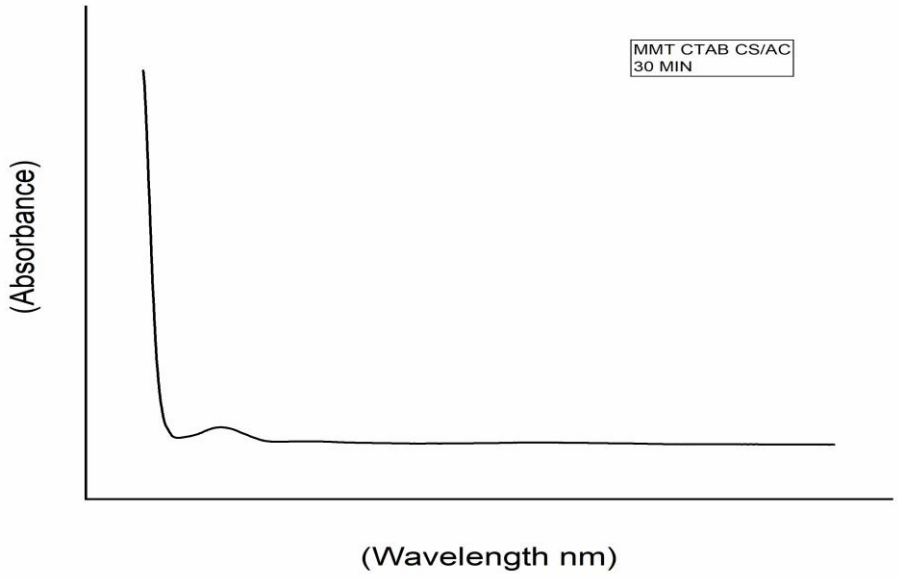

Fig.3.16 UV Visible spectrum of dye solution in MMT CTAB CS/AC Nanocomposite for 30 Min

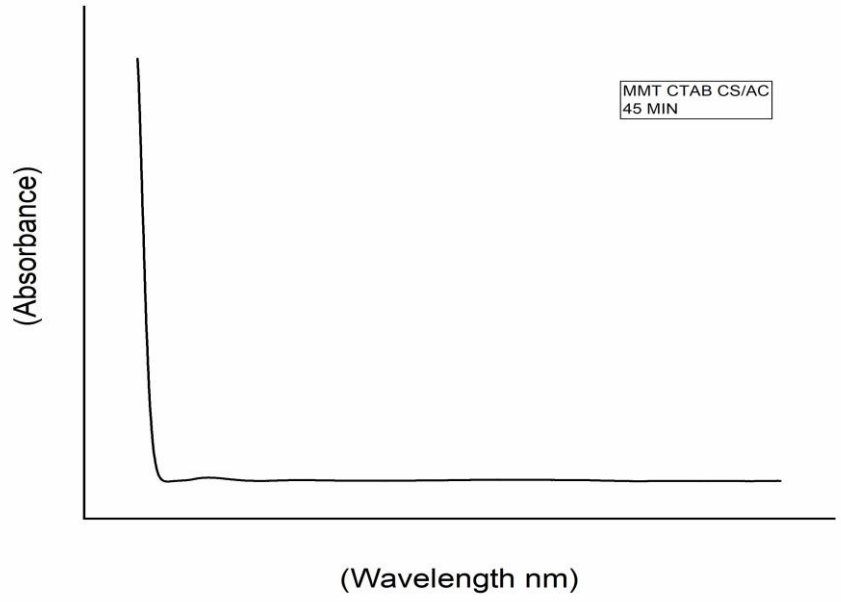

Fig.3.17 UV Visible spectrum of dye solution in MMT CTAB CS/AC Nanocomposite for 45 Min

Table 3.14 UV Visible Analysis of Dye solution in MMT-CTAB CS/AC nanocomposite at different time intervals

Sample	Wavelength (nm)	Absorbance
MMT-CTAB CS/AC for 15 Min	260	0.4180
MMT-CTAB CS/AC For 30 Min	260	0.1093
MMT-CTAB CS/AC For 45 Min	260	0.0537

In comparison of UV Data obtained for Dye and MMT CTAB Cinnamic CS/AC and MMT-CTAB CS/AC nanocomposites is listed in tables 3.12, 3.13, 3.14

The adsorption efficiency of the nanocomposites toward alizarin red dye was evaluated by monitoring their absorbance at 260 nm using UV–Vis spectroscopy. The results clearly demonstrate the superior adsorption capability of the prepared MMT–CTAB CS/AC nanocomposites.

The pure dye solution exhibited an absorbance of 0.9407 Abs. In contrast, the MMT-CTAB CS/AC composite showed a progressive decrease in absorbance over time, with values of 0.4180 Abs after 15 minutes, 0.1093 Abs after 30 minutes, and 0.0537 Abs after 45 minutes. This consistent reduction in absorbance confirms the effective removal of dye from the aqueous solution.

The remarkable adsorption performance can be attributed to the increased interlayer spacing (d-spacing) within the MMT CS/AC nanocomposites. The expansion of the clay layers enhances surface area and improves interlayer accessibility, thereby providing more active sites for dye

molecule interaction and adsorption. The gradual decrease in absorbance over time further indicates continuous and efficient dye uptake.

In contrast, the MMT– CTAB Cinnamic acid CS/AC nanocomposite displayed an increase in absorbance. This behaviour may be explained by the relatively weak interaction between cinnamic acid and the MMT clay layers. During stirring, partial leaching of cinnamic acid into the aqueous medium likely occurred, contributing to the observed rise in absorbance. This suggests reduced structural stability and lower adsorption efficiency compared to the CTAB-modified composite.

Chapter 4

Conclusions

The MMT–CTAB–cinnamic acid CS/AC nanocomposite and MMT-CTAB CS/AC nanocomposite was successfully synthesized and comprehensively characterized. The synthesis involved the preparation of a separate CS/AC composite, modification of MMT clay using CTAB–cinnamic acid, and modification of MMT using CTAB alone. The modified MMT was subsequently incorporated into the CS/AC composite, and the mixture was subjected to sonication to ensure uniform dispersion and formation of a homogeneous nanocomposite. The obtained nanocomposite exhibited an exfoliated clay structure, as expected, providing a high surface area and increased availability of active sites, thereby enhancing the adsorption capacity of the clay.

Fourier Transform Infrared (FTIR) spectroscopy revealed significant interactions among the composite components. The characteristic absorption bands corresponding to functional groups of MMT, chitosan, cinnamic acid, CTAB, and activated carbon were carefully examined. The presence of hydroxyl (–OH) and amide (–NH) stretching vibrations confirmed the physical blending and successful incorporation of the constituents. The absence of newly formed peaks indicated that no chemical reactions occurred during synthesis, thereby maintaining the structural integrity of the nanocomposite.

X-ray diffraction (XRD) analysis confirmed the intercalation of MMT within the polymer matrix. A noticeable increase in basal spacing and partial exfoliation of MMT layers was observed in the CS/AC–MMT nanocomposite, demonstrating effective insertion of polymer chains between the clay galleries.

Overall, the characterization results confirm the successful fabrication of both CS/AC–MMT–CTAB–cinnamic acid and CS/AC–MMT–CTAB nanocomposites. The combined FTIR and XRD findings demonstrate efficient incorporation of MMT into the polymer matrix, improved clay dispersion, and enhanced structural compatibility among the composite components.

The absorption efficiency of MMT-CTAB CS/AC Nanocomposite was analyzed using UV-Visible spectroscopy at a wavelength of 260 nm. The UV Visible analysis confirms the remarkable adsorption efficiency of MMT-CTAB CS/AC nanocomposite in removing the Alizarin red dye from aqueous solutions. The spectroscopy analysis of pure dye indicated an absorbance of 0.9407 Abs, whereas the MMT-CTAB nanocomposite showed an evident reduction in absorbance; here, the values are 0.4180 Abs in 15 mins, 0.1093 Abs in 30 mins and 0.0537 Abs in 45 mins. These observed values highlight the stability and effectiveness of this nanocomposite in dye removal. The enhanced absorption is due to the increased d-spacing of nanocomposites, making it an exfoliated structure with enhanced interlayer accessibility, surface exposure, porosity and more active interaction sites. These structural characteristics contribute to its exceptional adsorption capability.

The UV–Visible spectroscopy analysis revealed that the MMT–CTAB Cinnamic Acid CS/AC nanocomposite exhibited comparatively lower adsorption efficiency in the removal of Alizarin red dye from aqueous solutions. Unlike the MMT–CTAB CS/AC nanocomposite, which showed a significant reduction in absorbance over time, the MMT–Cinnamic Acid–modified system demonstrated an increase in absorbance values. The presence of cinnamic acid within the matrix appears to interfere with the active adsorption sites, thereby reducing effective dye interaction and limiting the overall removal efficiency.

The reduced performance of the MMT–CTAB Cinnamic acid CS/AC nanocomposite can be attributed to the weak intermolecular forces between cinnamic acid and the composite structure. Due to insufficient binding strength, cinnamic acid molecules tend to leach out into the aqueous medium during the stirring process. Once released, cinnamic acid absorbs UV radiation, contributing to an apparent increase in absorbance values and masking the actual dye removal efficiency. Furthermore, the partial detachment of cinnamic acid may disrupt the structural integrity and interlayer interactions of the nanocomposite, decreasing porosity, surface accessibility, and the number of effective active sites. These factors collectively confirm the inefficiency and reduced stability of the MMT–CTAB Cinnamic acid CS/AC nanocomposite for wastewater treatment applications.

The characterization studies confirmed the successful synthesis of MMT-CTAB CS/AC Nanocomposite and MMT-CTAB Cinnamic CS/AC Nanocomposite. The FT-IR and XRD analysis show the viable incorporation of CTAB, Cinnamic acid, Chitosan and Activated carbon

within the MMT clay layers. The UV-Visible spectroscopy indicated the stability and efficiency of MMT-CTAB CS/AC Nanocomposite for dye absorption. Based on our experimental results, it confirms that the MMT-CTAB CS/AC Nanocomposite is a viable and efficient material for waste water treatment applications.

References

1. Sonune A, Ghate R. Developments in wastewater treatment methods. Desalination [Internet]. 2004 Aug;167:55–63. Available from: https://linkinghub.elsevier.com/retrieve/pii/S0011916404003558
2. Tkaczyk A, Mitrowska K, Posyniak A. Synthetic organic dyes as contaminants of the aquatic environment and their implications for ecosystems: A review. Sci Total Environ [Internet]. 2020 May;717:137222. Available from: https://linkinghub.elsevier.com/retrieve/pii/S0048969720307324
3. Garg A, Chopra L. Dye Waste: A significant environmental hazard. Mater Today Proc [Internet]. 2022;48:1310–5. Available from: https://linkinghub.elsevier.com/retrieve/pii/S2214785321057886
4. Bhatia D, Sharma NR, Singh J, Kanwar RS. Biological methods for textile dye removal from wastewater: A review. Crit Rev Environ Sci Technol [Internet]. 2017 Oct 2;47(19):1836–76. Available from: https://www.tandfonline.com/doi/full/10.1080/10643389.2017.1393263
5. Bal G, Thakur A. Distinct approaches of removal of dyes from wastewater: A review. Mater Today Proc [Internet]. 2022;50:1575–9. Available from: https://linkinghub.elsevier.com/retrieve/pii/S2214785321059162
6. Gómez V, Larrechi MS, Callao MP. Kinetic and adsorption study of acid dye removal using activated carbon. Chemosphere [Internet]. 2007 Oct;69(7):1151–8. Available from:

https://linkinghub.elsevier.com/retrieve/pii/S0045653507004614

7. Foo KY, Hameed BH. An overview of dye removal via activated carbon adsorption process. Desalin Water Treat [Internet]. 2010 Jul;19(1–3):255–74. Available from: https://linkinghub.elsevier.com/retrieve/pii/S1944398624182161
8. Lu PJ, Lin HC, Yu WT, Chern JM. Chemical regeneration of activated carbon used for dye adsorption. J Taiwan Inst Chem Eng [Internet]. 2011 Mar;42(2):305–11. Available from: https://linkinghub.elsevier.com/retrieve/pii/S1876107010001045
9. Bergaya F, Lagaly G. Chapter 1 General Introduction: Clays, Clay Minerals, and Clay Science. In 2006. p. 1–18. Available from: https://linkinghub.elsevier.com/retrieve/pii/S1572435205010019
10. Chapter 1 The Clay Minerals. In 1979. p. 3–36. Available from: https://linkinghub.elsevier.com/retrieve/pii/S0166248108701120
11. Schoonheydt RA, Johnston CT. The surface properties of clay minerals. In: Layered Mineral Structures and their Application in Advanced Technologies [Internet]. Mineralogical Society of Great Britain and Ireland; 2011. p. 335–70. Available from: https://pubs.geoscienceworld.org/minersoc/books/edited-volume/2523/chapter/142061510/The-surface-properties-of-clay-minerals
12. Murray HH. Chapter 2 Structure and Composition of the Clay Minerals and their Physical and Chemical Properties. In 2006. p. 7–31. Available from: https://linkinghub.elsevier.com/retrieve/pii/S1572435206020022
13. Adeyemo AA, Adeoye IO, Bello OS. Adsorption of dyes using different types of clay: a review. Appl Water Sci [Internet]. 2017;7(2):543–68. Available from: https://doi.org/10.1007/s13201-

015-0322-y

14. Wang YH, Siu WK. Structure characteristics and mechanical properties of kaolinite soils. I. Surface charges and structural characterizations. Can Geotech J [Internet]. 2006 Jun 1;43(6):587–600. Available from: http://www.nrcresearchpress.com/doi/10.1139/t06-026
15. Odom IE. Smectite clay minerals: properties and uses. Philos Trans R Soc London [Internet]. 1984 Jun 14;311(A311):391–409. Available from: https://doi.org/10.1098/rsta.1984.0036
16. Wang W, Wang A. Vermiculite Nanomaterials: Structure, Properties, and Potential Applications. In: Nanomaterials from Clay Minerals [Internet]. Elsevier; 2019. p. 415–84. Available from: https://linkinghub.elsevier.com/retrieve/pii/B9780128145333000090
17. Carmignano O, Vieira S, Brandão PR, Bertoli A, Lago R. Serpentinites: Mineral Structure, Properties and Technological Applications. J Braz Chem Soc [Internet]. 2020; Available from: http://jbcs.sbq.org.br/audiencia_pdf.asp?aid2=5720&nomeArquivo=2019-0200RV.pdf
18. Mielenz RC, King ME. Physical-Chemical Properties and Engineering Performance of Clays. Clays clay Technol (National Conf Clays Clay Technol [Internet]. 1955 Jul 1;1:196–254. Available from: https://www.cambridge.org/core/product/identifier/S2640937200000210/type/journal_article
19. Abdulabbas AA. Clay basics and their physical and chemical properties: Review Paper. Available from: r
20. Ross CS, Shannon E V. THE MINERALS OF BENTONITE AND

RELATED CLAYS AND THEIR PHYSICAL PROPERTIES 1. J Am Ceram Soc [Internet]. 1926 Feb 2;9(2):77–96. Available from: https://ceramics.onlinelibrary.wiley.com/doi/10.1111/j.1151-2916.1926.tb18305.x

21. Tournassat C, Bourg IC, Steefel CI, Bergaya F. Surface Properties of Clay Minerals. In 2015. p. 5–31. Available from: https://linkinghub.elsevier.com/retrieve/pii/B9780081000274000012

22. Schoonheydt RA, Johnston CT. Chapter 3 Surface and Interface Chemistry of Clay Minerals. In 2006. p. 87–113. Available from: https://linkinghub.elsevier.com/retrieve/pii/S1572435205010032

23. Hojiyev R, Ersever G, Karaağaçlıoğlu İE, Karakaş F, Boylu F. Changes on montmorillonite characteristics through modification. Appl Clay Sci [Internet]. 2016 Jul;127–128:105–10. Available from: https://linkinghub.elsevier.com/retrieve/pii/S0169131716301430

24. Mose BR, Maranga SM. A Review on Starch Based Nanocomposites for Bioplastic Materials. Former part J Mater Sci Eng. 2011;1:239–45.

25. Yaghmaeiyan N, Mirzaei M, Delghavi R. Montmorillonite clay: Introduction and evaluation of its applications in different organic syntheses as catalyst: A review. Results Chem [Internet]. 2022 Jan;4:100549. Available from: https://linkinghub.elsevier.com/retrieve/pii/S2211715622002685

26. Tyagi B, Chudasama CD, Jasra R V. Determination of structural modification in acid activated montmorillonite clay by FT-IR spectroscopy. Spectrochim Acta Part A Mol Biomol Spectrosc [Internet]. 2006 May;64(2):273–8. Available from:

https://linkinghub.elsevier.com/retrieve/pii/S1386142505003677

27. Ijagbemi CO, Baek MH, Kim DS. Montmorillonite surface properties and sorption characteristics for heavy metal removal from aqueous solutions. J Hazard Mater [Internet]. 2009 Jul;166(1):538–46. Available from: https://linkinghub.elsevier.com/retrieve/pii/S0304389408017469
28. Maliki S, Sharma G, Kumar A, Moral-Zamorano M, Moradi O, Baselga J, et al. Chitosan as a Tool for Sustainable Development: A Mini Review. Polymers (Basel) [Internet]. 2022 Apr 5;14(7):1475. Available from: https://www.mdpi.com/2073-4360/14/7/1475
29. Alsohaimi IH, Alhumaimess MS, Hassan HMA, Reda M, Aldawsari AM, Chen Q, et al. Chitosan Polymer Functionalized-Activated Carbon/Montmorillonite Composite for the Potential Removal of Lead Ions from Wastewater. Polymers (Basel) [Internet]. 2023 May 5;15(9):2188. Available from: https://www.mdpi.com/2073-4360/15/9/2188
30. Unagolla JM, Adikary SU. Adsorption characteristics of cadmium and lead heavy metals into locally synthesized Chitosan Biopolymer. Trop Agric Res. 2015;26(2):395.
31. Aranaz I, Alcántara AR, Civera MC, Arias C, Elorza B, Heras Caballero A, et al. Chitosan: An Overview of Its Properties and Applications. Polymers (Basel) [Internet]. 2021 Sep 24;13(19):3256. Available from: https://www.mdpi.com/2073-4360/13/19/3256
32. Wang W, Meng Q, Li Q, Liu J, Zhou M, Jin Z, et al. Chitosan Derivatives and Their Application in Biomedicine. Int J Mol Sci [Internet]. 2020 Jan 12;21(2):487. Available from: https://www.mdpi.com/1422-0067/21/2/487

33. I.P. S, P.I. S. New Conceptions about Structure Formation of Biopolymers. Biotechnology of Biopolymers. 2011.
34. Ikram S, Islamia JM. Chitosan & its derivatives: A review in recent innovations. Int J Pharm Sci Res [Internet]. 2015;6(1):14–30. Available from: http://ijpsr.com/bft-article/chitosan-its-derivatives-a-review-in-recent-innovations-2/
35. Nechita P. Applications of chitosan in wastewater treatment, biological activities and application of marine polysaccharides. Biol Act Appl Mar Polysaccharides. 2017;209–28.
36. Riaz Rajoka MS, Zhao L, Mehwish HM, Wu Y, Mahmood S. Chitosan and its derivatives: synthesis, biotechnological applications, and future challenges. Appl Microbiol Biotechnol [Internet]. 2019 Feb 3;103(4):1557–71. Available from: http://link.springer.com/10.1007/s00253-018-9550-z
37. Zhang M, Zhang F, Li C, An H, Wan T, Zhang P. Application of Chitosan and Its Derivative Polymers in Clinical Medicine and Agriculture. Polymers (Basel) [Internet]. 2022 Feb 28;14(5):958. Available from: https://www.mdpi.com/2073-4360/14/5/958
38. Heidarinejad Z, Dehghani MH, Heidari M, Javedan G, Ali I, Sillanpää M. Methods for preparation and activation of activated carbon: a review. Environ Chem Lett [Internet]. 2020 Mar 4;18(2):393–415. Available from: http://link.springer.com/10.1007/s10311-019-00955-0
39. Bhatnagar A, Hogland W, Marques M, Sillanpää M. An overview of the modification methods of activated carbon for its water treatment applications. Chem Eng J [Internet]. 2013 Mar;219:499–511. Available from: https://linkinghub.elsevier.com/retrieve/pii/S1385894712016786

40. Suzuki M. Activated carbon fiber: Fundamentals and applications. Carbon N Y [Internet]. 1994;32(4):577–86. Available from: https://linkinghub.elsevier.com/retrieve/pii/0008622394900752
41. Caturla F, Molina-Sabio M, Rodríguez-Reinoso F. Preparation of activated carbon by chemical activation with ZnCl2. Carbon N Y [Internet]. 1991;29(7):999–1007. Available from: https://linkinghub.elsevier.com/retrieve/pii/000862239190179M
42. Guo B, Chang L, Xie K. Adsorption of Carbon Dioxide on Activated Carbon. J Nat Gas Chem [Internet]. 2006 Sep;15(3):223–9. Available from: https://linkinghub.elsevier.com/retrieve/pii/S1003995306600303
43. Shafeeyan MS, Daud WMAW, Houshmand A, Shamiri A. A review on surface modification of activated carbon for carbon dioxide adsorption. J Anal Appl Pyrolysis [Internet]. 2010 Nov;89(2):143–51. Available from: https://linkinghub.elsevier.com/retrieve/pii/S0165237010001063
44. Julien F, Baudu M, Mazet M. Relationship between chemical and physical surface properties of activated carbon. Water Res [Internet]. 1998 Nov;32(11):3414–24. Available from: https://linkinghub.elsevier.com/retrieve/pii/S0043135498001092
45. Dias JM, Alvim-Ferraz MCM, Almeida MF, Rivera-Utrilla J, Sánchez-Polo M. Waste materials for activated carbon preparation and its use in aqueous-phase treatment: A review. J Environ Manage [Internet]. 2007 Dec;85(4):833–46. Available from: https://linkinghub.elsevier.com/retrieve/pii/S0301479707002964
46. Viseras C, Aguzzi C, Cerezo P, Bedmar MC. Biopolymer–clay nanocomposites for controlled drug delivery. Mater Sci Technol [Internet]. 2008 Sep 1;24(9):1020–6. Available from:

https://journals.sagepub.com/doi/10.1179/174328408X341708

47. Aranda P, Darder M, Fernández-Saavedra R, López-Blanco M, Ruiz-Hitzky E. Relevance of polymer– and biopolymer–clay nanocomposites in electrochemical and electroanalytical applications. Thin Solid Films [Internet]. 2006 Jan;495(1–2):104–12. Available from: https://linkinghub.elsevier.com/retrieve/pii/S0040609005013933
48. Darder M, Colilla M, Ruiz-Hitzky E. Biopolymer−Clay Nanocomposites Based on Chitosan Intercalated in Montmorillonite. Chem Mater [Internet]. 2003 Oct 1;15(20):3774–80. Available from: https://pubs.acs.org/doi/10.1021/cm0343047
49. Darder M, Colilla M, Ruiz-Hitzky E. Chitosan–clay nanocomposites: application as electrochemical sensors. Appl Clay Sci [Internet]. 2005 Jan;28(1–4):199–208. Available from: https://linkinghub.elsevier.com/retrieve/pii/S016913170400081X
50. Orta M del M, Martín J, Santos JL, Aparicio I, Medina-Carrasco S, Alonso E. Biopolymer-clay nanocomposites as novel and ecofriendly adsorbents for environmental remediation. Appl Clay Sci [Internet]. 2020 Nov;198:105838. Available from: https://linkinghub.elsevier.com/retrieve/pii/S0169131720304038
51. Perotti GF, Tronto J, Bizeto MA, Izumi CMS, Temperini MLA, Lugão AB, et al. Biopolymer-Clay Nanocomposites: Cassava Starch and Synthetic Clay Cast Films. J Braz Chem Soc [Internet]. 2013; Available from: https://jbcs.sbq.org.br/audiencia_pdf.asp?aid2=3855&nomeArquivo=v25n2a15.pdf
52. Rhim JW, Ng PKW. Natural Biopolymer-Based Nanocomposite Films for Packaging Applications. Crit Rev Food Sci Nutr

[Internet]. 2007 Apr 26;47(4):411–33. Available from: https://www.tandfonline.com/doi/full/10.1080/10408390600846366

53. Fatyeyeva K, Chappey C, Marais S. Biopolymer/clay nanocomposites as the high barrier packaging material: recent advances. In: Food Packaging [Internet]. Elsevier; 2017. p. 425–63. Available from: https://linkinghub.elsevier.com/retrieve/pii/B9780128043028000133